NASA CONTRACTOR REPORT

NASA CR-2780

NASA CR-2780

STUDY OF PHOTON CORRELATION TECHNIQUES FOR PROCESSING OF LASER VELOCIMETER SIGNALS

William T. Mayo, Jr.

Prepared by
SCIENCE APPLICATIONS, INC.
Atlanta, Ga. 30339
for Langley Research Center

NATIONAL AERONAUTICS AND SPACE ADMINISTRATION • WASHINGTON, D. C. • FEBRUARY 1977

1. Report No.	2. Government Accession No.	3. Recipient's Catalog No.
NASA CR-2780		

4. Title and Subtitle	5. Report Date
Study of Photon Correlation Techniques for Processing of Laser Velocimeter Signals	February 1977
	6. Performing Organization Code

7. Author(s)	8. Performing Organization Report No.
William T. Mayo, Jr.	
	10. Work Unit No.

9. Performing Organization Name and Address	11. Contract or Grant No.
Science Applications, Inc. Atlanta, GA 30339	NAS1-13737
	13. Type of Report and Period Covered
	Contractor Report

12. Sponsoring Agency Name and Address	14. Army Project No.
National Aeronautics and Space Administration Washington, DC 20546 and U.S. Army Air Mobility R&D Laboratory Moffett Field, CA 94035	1F161102A35B

15. Supplementary Notes

The contract research effort which has led to the results in this report was financially supported by USAAMRDL (Langley Directorate).

Langley technical monitor: William W. Hunter, Jr. Final report.

16. Abstract

The objective of this work was to provide the theory and a system design for a new type of photon-counting processor for low-level Dual Scatter laser velocimeter (LV) signals which would be capable of both the first-order measurements of mean-flow and turbulence-intensity and also the second order time statistics: cross-correlation, auto-correlation, and related spectra. A general Poisson process model for low-level LV signals and noise which is valid from the photon-resolved regime all the way to the limiting case of non-stationary Gaussian noise was used. Computer simulation algorithms and higher order statistical moment analysis of Poisson processes have been derived and applied to the analysis of photon correlation techniques. A system design using a unique Dual Correlate and Subtract frequency discriminator technique is postulated and analyzed. Expectation analysis indicates that the objective measurements are feasible. Error analysis for the mean-flow case indicates that practical transonic wind tunnel measurements are possible with 100-1000 times less light than is required for burst-counter processors. A system design for a new high-speed photon processor for LV signals is provided.

17. Key Words (Suggested by Author(s))	18. Distribution Statement
Data processing Laser doppler velocimeter Digital systems Velocity measurement	Unclassified-Unlimited Subject Category 60

19. Security Classif. (of this report)	20. Security Classif. (of this page)	21. No. of Pages	22. Price*
Unclassified	Unclassified	110	$5.25

*For sale by the National Technical Information Service, Springfield, Virginia 22161

STUDY OF PHOTON CORRELATION TECHNIQUES FOR PROCESSING OF LASER VELOCIMETER SIGNALS

By William T. Mayo, Jr.

Summary

The objective of this contract was to provide the theory and system design for a new type of photon-counting processor for low-level Dual Scatter laser velocimeter (LV) signals which would be capable of both the first-order measurements of mean-flow and turbulence-intensity and also the second order time statistics: cross-correlation, auto-correlation, and related spectra.

This report provides a general Poisson process model for low-level LV signals and noise which is valid from the photon-resolved regime all the way to the limiting case of non-stationary Gaussian noise. Computer simulation algorithms and higher order statistical moment analysis of Poisson processes have been derived and applied to the analysis of photon correlation techniques. A Dual Correlate and Subtract frequency discriminator technique is postulated and analyzed. Expectation analysis indicates that the objective measurements are feasible. Error analysis for the mean-flow case indicates that practical transonic wind tunnel measurements are possible with 100-1000 times less light than is required for burst-counter processors. A system design for a new high-speed photon processor for LV signals is provided.

CONTENTS

LIST OF ILLUSTRATIONS

Figure

LIST OF TABLES

INTRODUCTION

The Problem

Classical laser velocimeter (LV) electronic signal processing techniques are sometimes inadequate for detection of light scattered by small scattering particles which are required for following fluid motions. In other situations detection of larger scattering particles is difficult due to limited system sensitivity. Photon counting techniques offer improved system sensitivity by allowing velocity measurements to be made even when there are insufficient signal photons available to define the classical scattering signal. Such techniques are thus applicable when the presently used classical burst-counter and frequency tracker-techniques are not.

The general objective of this contract was to provide the system design for a new type of photon-counting processor for low-level Dual Scatter LV signals which would be capable of both the first-order measurements of mean-flow and turbulence-intensity and also the second order time statistics: cross correlation, auto-correlation, and related spectra. This was to be accomplished by extending the preliminary feasibility analysis developed under a brief NASA Langley sponsored study* in early 1974. In addition to theory, the system design would incorporate judgement based on experience in the experimental hardware development [1] of a related, but simpler, photon-counting processing system designed and constructed for the U.S.A.F. Arnold Engineering Development Center to measure mean-flow velocities.

---

*The final report for that study (Contract NAS1-13140) was informal and not disseminated. This report contains revised versions of all the necessary mathematics.

Signal modeling.- Earlier modeling efforts have treated LV signals for which the noise could be considered as additive independent, stationary, and Gaussian [2,3,4,5]. This is the limiting case of stationary Poisson shot noise which occurs for visible light photodetection when a steady light source such as a heterodyne reference beam [2] or high background light level [3] dominates the signal. In a recent simulation of low-level dual scatter signals, the accuracy of the noise model was

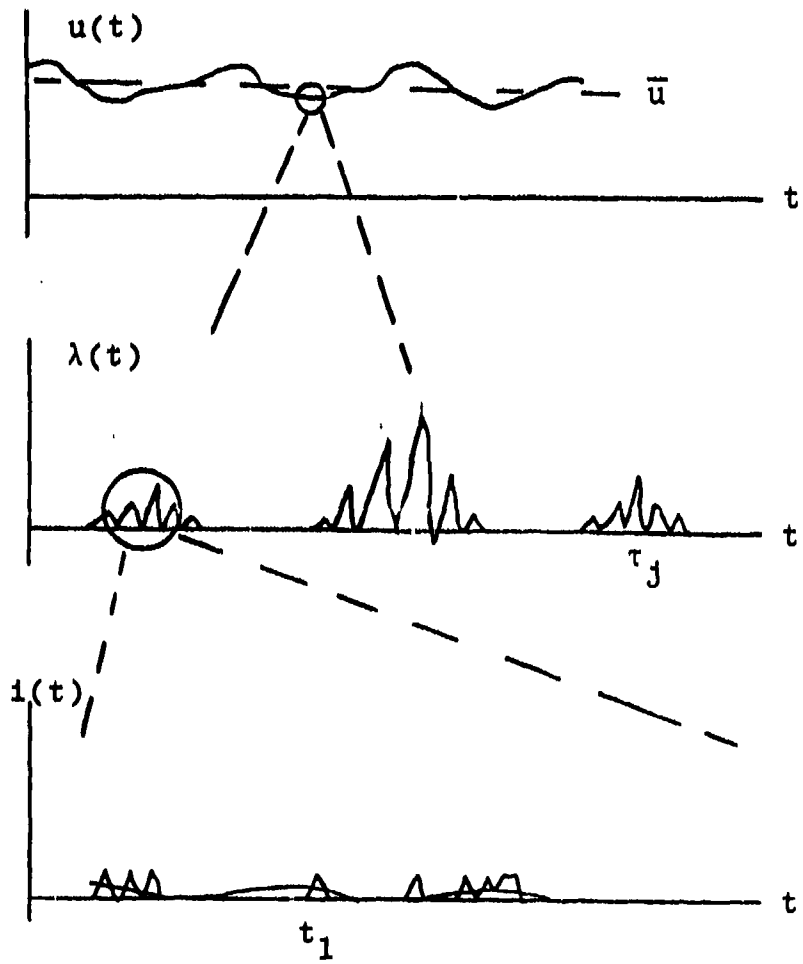

Figure 1. Triply Stochastic Nature of Low-Level LV Signals: Turbulence, Bursts, and Photo electron Pulses.

extended by treating it as a nonstationary Gaussian process whose variance is proportional to the incident optical power.*

When we discuss "noise" in LV signal detection we are usually referring to the variation of the electronically detected signal with respect to a scaled version of the classical optical (power) signal incident on the PMT. In a general analysis the classical LV signals are also random processes due to the random amplitudes and the arrival times of the signal bursts. Mayo [2] and Adrian [7] have treated these signals as a Poisson process for steady flow, and Durrani [4] and George [8] have treated them for the turbulent flow case as Gaussian in the limit of high particle number density. A new book by Snyder [9] treats generalized Poisson processes in great detail. Papoulis [10] provides a good introductory treatment. Snyder treats "doubly stochastic Poisson processes." These are inhomogeneous (nonstationary) Poisson processes for which the rate function is a random process. Such a description is appropriate either for the classical LV signal bursts with the random turbulent flow affecting the rate of burst occurrence or for the single photoelectron pulses from the PMT with the random classical bursts as the rate function. Clearly, when taken from the turbulence to the photo-electron pulses, a dual-scatter LV signal is a "triply stochastic" filtered Poisson process [11]. This three level nature of the signals is illustrated by Figure 1.

Classical signals and burst counters. Presently accepted burst-counter and frequency-tracker LV processors were developed by analogy with wide-band frequency modulation (FM) and radar receivers. For FM and radar applications frequency detection (zero-crossing) circuits generally require about 10 db signal power to noise power ratio within the bandwidth of the system filters. The signals in such cases are continuous and the noise

*Modified version of noise model described in [6].

is stationary and Gaussian. Comments by several speakers at the 1975 Minnesota LDA Symposium indicated that they had experimentally determined that their burst counter LV signal processors failed significantly when the signal power to noise power ratio (during a burst) was less than 10 db. This 10 db condition occurs when there are approximately 10 or more photoelectron pulses per electronic response time τ_h. This response time is rise time or pulse width in the case of low-pass filter. We have also defined this signal level as the lowest value of the "Gaussian" signal regime wherein the photomultiplier current can be modeled as the classical signal plus nonstationary Gaussian noise; (although neither Snyder [9] or Papoulis [10] give any helpful rules as to when this asymptotic approximation is valid). For lower signal power the signals must be treated as Poisson.

Photon resolved signals and photon counting.- A radically different approach to LV signal detection has been taken by Pike, Oliver, Jakeman, and others. Photon counting techniques were developed for use with low-level photon resolved signals. The summary results of several years of development of the single-clipping real-time photon correlator were described by Oliver and Jakeman in a recent book [12]. Dr. Pike described the application of photon-correlation to the processing of LV signals at the 1972 Purdue conference [13]. The presentation was apparently not received well by many attendees from the United States and little has been done in this country with the development of photon counting techniques until recently. Increased interest was shown by attendees of the 1974 Purdue Conference.

One reason that the single-clipping correlator has been slow to acceptance in this country is that the original theory for its use was based on the assumption of many scatterers in the probe volume with the central limit theorem invoked to

render the statistics of the scattered electric fields Gaussian. Since this assumption is known not to predominate in many applications of fringe-type LV systems in air, none of the first theory for a single-clipping correlator was directly applicable. Another problem with the existing commercial correlators for high-speed air flow besides speed (minimum time resolution of 50 nsec) is the lack of any straightforward way to extend the concept to the determination of flow time statistics such as correlations and power spectra. The system proposed in this report addresses this latter deficiency as well as eliminating the problems of interpretation of single-clipping by using full multiplication.

Several recent references provide additional valuable background information on photon correlation. Durrani and Greated [14] provide a derivation of the expected value of a photon correlation from single particle (Poisson) signals. Birch et al. [15] have made experimental measurements in turbulent jet flows with skewed probability density functions. Abbiss et al. [16] also provide an analysis which shows that in some cases the Fourier transform of the correlogram may be interpreted as the probability density of the fluid velocity component.* Durrani and Greated [17] have investigated the use of some of the newer spectral estimation techniques which allow greater resolution from the limited number of data points in a typical correlogram. Finally, the reader should be aware that a new photon correlator instrument has been developed which was described by C. Fog [18] but the minimum time resolution interval is 160 nsec which is rather slow for high speed wind tunnel applications. (It was used for atmospheric studies.)

---

*We do not believe this will be a good approximation in many practical cases. This is discussed in a later section.

Burst rate/amplitude distributions.- The statistical distribution of the classical burst amplitudes and the rate of occurrence versus amplitude are very significant in the characterization of any LV signal processor. It is generally accepted, for example, that the optimum rate of occurrence of bursts for a burst counter is less than the inverse burst duration (non-overlapping bursts.) It is also generally known that the error check circuits cause a burst counter to emphasize larger amplitude (good signal to noise ratio) signals. On the other hand, a photon counting processor must emphasize the lower amplitude signals in a distribution; the higher amplitude signals would produce only a single threshold crossing and otherwise be neglected by the system. It is therefore not possible to compare two different types of signal processors without knowing the signal amplitude distributions and the processor behavior as a function of burst amplitude and other factors. Finally, in order to relate processor behavior to a specified particle size distribution, one must first relate the particle size distribution to the burst amplitude distributions and then do all the other things already discussed.

During the initial phases of our recent work for the USAF Arnold Center we addressed such questions as are suggested by the above statements both with theoretical models and with experimental measurements of burst rate/amplitude distributions for natural laboratory (unfiltered and unseeded) air. The reader is referred to the final report [1] for details. The following is one of the concluding paragraphs of that report:

> The statistical distribution of the amplitudes and rates of occurrence of classical bursts has been shown to be central in the problem of specifying or predicting the data rates and errors from any type of LV signal processor. Differential and cumulative rate/amplitude distributions have been formulated and analyzed theoretically and have been measured experimentally for an argon backscatter LV system. The results indicate that, for the data obtained, the smaller aerosols contribute

more to the photon correlation accumulator than the larger ones. For the data measured, there would have been available less than 300 signals per second adequate in magnitude to produce burst counter data from scatterers larger than 0.7 μm in diameter while there would have been over 100,000 signals per second producing photon resolved signals from 0.2 - 0.3 μm diameter particles.

Scope

In what follows we first develop general Poisson models for LV signals which include the non-stationary Poisson occurrence of photo-electron pulses and the random amplitude effects of both the photomultiplier tube and the particle scattering cross sections. Formulas are provided for conditional and unconditional moments including mean, variance, auto-covariance, and higher moments (Appendix A). These formulas are for signal current, but they become valid for photon counting by a suitable choice of the PMT output filter impulse response function.

The next section evaluates the theoretical expressions for a specific Gaussian burst LV waveform model. These results are used to obtain the expected value of a photon correlation estimate. In addition a Dual Correlate and Subtract estimator which behaves as a statistical frequency discriminator is postulated and analyzed. The following section is devoted to statistical error analysis of the mean flow estimation technique using the Dual Correlate approach. The section after that shows that the statistical frequency discriminator may be applied to the estimation of turbulence correlations even though the time history of the velocity fluctuations is not available except as a noisy randomly sampled waveform.

The results of the theoretical considerations and the experience we have had previously with the AEDC [1] hardware study were utilized in a system design which is provided in Appendix D. Appendix C is a derivation needed in the section on variability errors. Appendix B provides the theory and an example program for correct Poisson simulation of low-level LV signals for evaluation of electronic processor models.

LIST OF SYMBOLS

ENGLISH

B	bandwidth
$C_{ii}(t_1,t_2)$	autocovariance of i(t)
e	electronic charge
f	frequency
f_m	mean Doppler frequency
$f(\ )$	optical probe volume response function; pedastal function, peak amplitude normalized to unity
g_i	random single-photoelectron charge gain
h	Planck's constant
$h(t)$	impulse response of PMT and succeeding filters
$H(\omega)$	Fourier transform of h(t)
i	counting index
$i(t)$	photocurrent at anode or succeeding filter output
I	optical intensity
j	counting index
k	counting index
$m_i(t)$	time varying statistical mean current $\langle i(t) \rangle$
m_k	$n_k n_{k-p} - n_k n_{k-q}$ or other function of n_k
$\hat{M}_p$	photon correlation sum at delay $P\Delta\tau$
$\hat{M}_{pq}$	accumulation of $(p\Delta\tau, q\Delta\tau)$ for Dual Correlate Mode
$n(t_1,t_2)$	photoelectron count in interval (t_1,t_2)
n_k	photon count in $\Delta\tau$ interval about $k\Delta\tau$
N	number of time increments $\Delta\tau$ ($T = N\Delta\tau$)
N_f	number of fringes in the transmitter defined $1/e^2$ probe volume
N_t	total number of ΔT intervals in advanced concept operation
p	integer delay number in photon correlation; largest delay number in dual correlate and subtract
P_b	constant optical background power
$P(t)$	optical power incident on photocathode
q	integer value of delay

$\bar{r}_j$	location of the nearest approach of scatterer to center of probe volume
R	constant rate of signal bursts
R(t)	instantaneous rate of signal bursts
$R_\lambda(\tau)$	autocorrelation of $\lambda(t) = \langle\lambda(t)\lambda(t+\tau)\rangle$
s(t)	a generalized Poisson shot noise signal (Appendix A)
t	time
t_i	instants of photoelectron emission
T	total data collection time
T_m	inverse of mean Doppler frequency $1/f_m$
u(t)	time varying velocity component
U(t)	total velocity component
U	mean velocity component
$\bar{V}(t)$	vector velocity
w_o	$1/e^2$ intensity radius at beam waist
z(t)	Poisson impulse process

GREEK

α	integration dummy variable; also 1/e half-width of burst
β	integration dummy variable
$\delta(t)$	Dirac delta or unit impulse function
Δt	simulation time resolution interval
$\Delta\tau$	photon processor counting interval
ΔT	accumulation interval for second level correlation
ε	error
$\lambda(t)$	time varying mean rate of photoelectron pulses $\lambda(t) = \eta P(t)/h\nu$
λ_b	steady background photoelectron rate
λ_j	peak photoelectron rate (pedastal) from the jth scatterer
λ_o	optical wavelength
λ_s	mean signal photoelectron rate $\neq \langle\lambda_j\rangle$
η	product of photocathode quantum efficiency and dynode collection efficiency

ν	optical frequency
ρ	fractional turbulence intensity $\sigma_u/u \approx \sigma_\omega/\omega_m$
σ_ω	rms deviation of the radian Doppler frequencies from scatterers
$\sigma_i^2(t)$	time varying variance of i(t): $\langle(i(t) - \langle i(t)\rangle)^2\rangle$
τ	delay variable
τ_h	rise time or pulse width of low pass h(t)
τ_j	occurrence time for jth signal burst
θ	beam intersection angle; spherical declination angle from direction of incident light
ϕ	polar angle
μ	Poisson parameter
ω	Fourier transform variable or radian frequency
ω_j	random frequency of jth burst
ω_m	mean of random variable ω_j $(2\pi f_m)$

Special Notation

$\langle x \rangle$	statistical expectation of $x = \int_{-\infty}^{\infty} x\, p_x(x)dx$
$f(t)*g(t)$	convolution: $\int_{-\infty}^{\infty} f(\alpha)g(t-\alpha)d\alpha$
$\hat{}$	denotes an estimate of a statistical average

Poisson Models

The Signal Current.- The signal current from a photomultiplier tube (PMT) is modeled as inhomogeneous filtered Poisson random process (see Appendix A and also reference [19]) given by

$$i(t) = \sum_{-\infty}^{\infty} e g_i h(t - t_i) \tag{1}$$

where t_i = random time of the ith photoelectron
e = electronic charge
g_i = random charge gain of PMT
$h(t)$ = impulse response of PMT/filter system

The system response h(t) is obtained as a convolution of the PMT impulse response $h_p(t)$, the transmission line impulse response $h_t(t)$, and the linear filter impulse response $h_f(t)$

$$h(t) = h_p(t) * h_t(t) * h_f(t) \tag{2}$$

where the asterisk denotes the convolution integral:

$$f(t) * g(t) = \int_{-\infty}^{\infty} f(\alpha) g(t - \alpha) d\alpha \tag{3}$$

The superposition assumes operation in the linear range of the PMT electron multiplier. The use of the function $h_p(t)$ assumes that all single photo-electron pulses have the same shape except for amplitude. This neglects minor random shape variation.

The quantity which relates i(t) to the classical optical power is the statistical mean rate $\lambda(t)$ of occurrence of the randomly occurring photoelectron pulses. Thus

$$\lambda(t) = \frac{\eta P(t)}{h\nu} \tag{4}$$

where η = product of cathode quantum efficiency and the dynode collection efficiency

$h\nu$ = Photon energy

$P(t)$ = Classical optical power, including background light and a constant component for dark current.

The effects of dark current are included by adding an equivalent power P_d. The model could be made more exact by adding a separate dark pulse summation with a separate distribution of amplitudes which are distributed somewhat differently than g_i; but this distinction will not often be required in LV applications.

The previous material includes little which restricts it to LV signals. We now consider the form of $\lambda(t)$ which is also treated as a filtered Poisson process.

Superposition of classical single burst signals.- Rigorous electromagnetic theory analysis of the scattered fields from more than one scatterer in the probe volume shows [20] mixing terms in P(t), the classical power incident on the PMT. However, in typical dual-scatter systems, the diffraction limited spot size of the collecting lens is much smaller than the probe volume; conservation of energy arguments show that in such cases the number of scatterers in the probe volume may be much greater than unity with statistically negligible coherent mixing, regardless of the quality of the collecting lens [2]. This is significant even for LV systems which only trigger on isolated large signal bursts because we must also include in the model the effects of smaller scatterers which may exist at higher number density. We will take the position that at the PMT the classical power P(t) is the superposition of the backgrounhd light power and the power from individual scatterers without coherent mixing cross terms. This will be acceptable so long as the average number of scatterers in one diffraction limited resolution cell of the receiver is less than unity.

A second consideration concerns the background light. Even when we neglect coherent mixing of signals, there are fluctuations in the classical background power. Bertolotti [21] provides a review of these effects. Broadband background sources can be largely suppressed by the use of narrowband spatial and wave-length filters, but not always adequately enough for measurements from small scatterers. If the background is modulated (for example fluorescent lights) the mean value signal is easily removed by electronic filters, but the non-stationary noise is not. When the broadband background is "steady" there are actually significant classical fluctuations at rates up to the optical bandwidth. Bertolotti shows that when the optical filter bandwidth is much greater than the PMT electronic bandwidth, the photoelectron statistics behave as though the classical fluctuations did not exist (they are averaged out). Laser light scattered from windows is not broadband and may exhibit undesirable fluctuations. This background should be minimized, and its effects studied further.

The random process $\lambda(t)$.- With cognizance of the preceding discussion, we model P(t) as the summation of a constant background P_b which includes broadband, laser, and dark current sources and an inhomogeneous filtered Poisson signal process.

$$\frac{h\nu\lambda(t)}{\eta} = P(t) = \left[\lambda_b + \sum_{j=-\infty}^{\infty} \lambda_j f(t - \tau_j, \bar{V}_j, \bar{r}_j)\right]\frac{h\nu}{\eta} \qquad (5)$$

where τ_j = occurrence time of jth scatterer reaching $\bar{r}_j$,
λ_j = random peak amplitude parameter,
$\bar{V}_j$ = vector velocity of the jth scatterer,
$\bar{r}_j$ = location of nearest approach of the scatterer trajectory to the center of the probe volume, and
$f(t,\bar{V},\bar{r})$ = normalized optical system response function.

The notation in equation (5) explicitly shows that in general the shape of a burst (including signal period, signal envelope,

and pedestal) is a function of the scatterer vector velocity and trajectory location. The response also has random λ_j amplitude which depends on both trajectory and particle scattering cross section. In general the set of instants τ_j are independent Poisson random events whose instantaneous rate, R(t), is statistically correlated with the velocity vector.

Discussion of the model.- Equation (5) is cast in a general form which obscures certain details with generality. First it assumes that the velocity of a scatterer remains constant while in the probe volume with a value $\overline{V}(\tau_j,\overline{r}_j)$. The extended theory of filtered Poisson processes is sufficiently general to encompass the fact that the functional form of the optical response function $f(t,\overline{V},\overline{r})$ depends on two vector random variables.* However, Snyder [9] assumes that the vector random parameters are independent. We are not certain at the present time what the statistical dependence of the rate function R(t) on the velocity $\overline{V}(t)$ may imply, but no serious consequences will result with low turbulence flow.

Conditional Signal Statistics of the Photocurrent

At times the models for the systems analysis problem may be simplified until analytical methods are applicable. In these cases the use of conditional statistics will usually simplify the analysis. Papoulis [10] discusses the use of conditional statistics at length. We utilize this technique at length in a later section. Basically for a multilevel random process the technique consists of assuming the higher level random processes are known and deterministic, evaluating conditional expectations assuming the higher level processes, then evaluating the expectation of the result with respect to the higher level processes. First we will consider statistics of i(t) assuming the classical optical signal $\lambda(t)$ is known.

*Elementary shot noise theory is restricted to an impulse response function which is constant in shape.

Instantaneous mean, variance, autocovariance.- The result in Appendix A may be applied to determine the instantaneous mean, variance and auto-covariance of the signal. These are given in terms of the function $\lambda(t)$. The results are as follow:

$$m_i(t) = \langle i(t) \rangle = e\langle g_i \rangle \lambda(t) * h(t) \tag{6}$$

$$\sigma_i^2(t) = \langle (i(t) - \langle i(t) \rangle)^2 \rangle = e^2 \langle g_i^2 \rangle \lambda(t) * h^2(t) \tag{7}$$

$$C_{ii}(t_1, t_2) = \langle i(t_1) i(t_2) \rangle - \langle i(t_1) \rangle \langle i(t_2) \rangle \tag{8}$$

$$= e^2 \langle g_i^2 \rangle \int_{\infty}^{\infty} \lambda(\alpha) h(t_1 - \alpha) h(t_2 - \alpha) d\alpha$$

where < > denotes statistical expectation and where the asterisk again denotes the convolution integral. These results include the specification that $h_p(t)$, the impulse response of the PMT anode, have unit weight, i.e.,

$$\int_{-\infty}^{\infty} h_p(t) dt = 1 \tag{9}$$

in order to maintain conservation of charge. The functions $h_t(t)$ and $h_f(t)$ may include amplification or loss factors and need not have unity weight.

Conditional noise and SNR.- The concept of signal-to-noise ratio arose in communications theory when the "noise" was an additive stationary Gaussian random process totally characterized by a mean, mean-square deviation (variance), and a power spectral density. The ratio of the peak or average signal to the rms noise was a useful measure. The preceding equations show the mean-square deviation (variance) to be an instantaneous time function which is related to the classical signal. Observation of real LV signals on an oscilloscope display or computer

simulations such as that shown in Figure 2 show that the concept of signal-to-noise-ratio is not an adequate figure of merit without careful specification.

For an example SNR definition, we consider a low-pass PMT impulse response as a rectangular function:

$$h(t) = \frac{1}{\tau_h} \text{Rect } (t/\tau_h) \tag{10}$$

where

$$\begin{aligned} \text{Rect } (t) &= 1, \quad |t| \leq 0.5 \\ &= 0, \quad |t| > 0.5 \end{aligned} \tag{11}$$

If we now also assume that $\tau_h << T_m$ where T_m is the signal

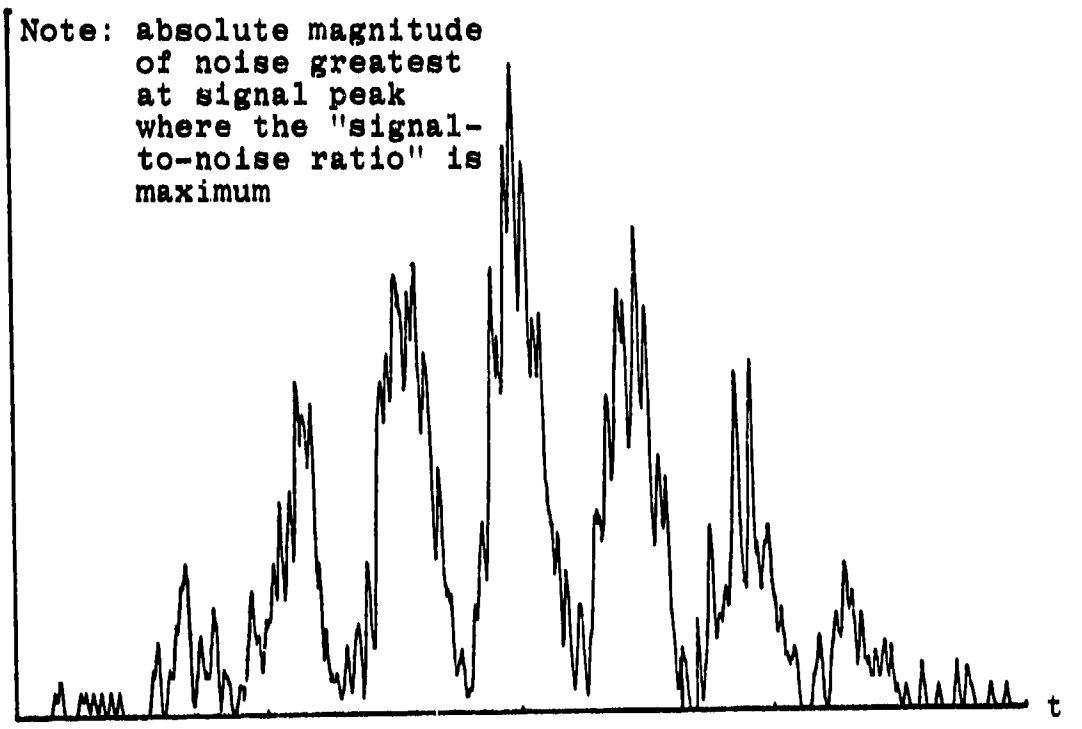

Figure 2. Computer Simulation of LV Signal using Algorithms similar to Appendix B. (By J. F. Meyers NASA Langley.)

period of interest, then we could obtain an instantaneous SNR from equations (6) and (7) as

$$SNR(t) = m_i^2(t)/\sigma_i^2(t) = \langle g_i\rangle^2\lambda^2(t)/\langle g_i^2\rangle\ \lambda(t)/\tau_h \qquad (12)$$

$$= \frac{\langle g_i\rangle^2}{\langle g_i^2\rangle}\ \lambda(t)\tau_h$$

where the quantity $\langle g_i\rangle^2/\langle g_i^2\rangle$ is typically between 0.5* and 1.0 with magnitude depending on the relative variance of the PMT single photoelectron pulse gain. For an ideal tube the quantity $\lambda(t)\tau_h$ would be the instantaneous SNR. This is not useful since it is a time function instead of a number.

As an alternative, we may take the local time average of the SNR given by (12) over a single cycle near the peak of the pedastal. This would give, for an ideal PMT,

$$SNR_{AVpeak} \approx \lambda_j\tau_h \qquad (13)$$

where λ_j is the peak value of the pedastal of the jth signal burst, if we assume sparse non-overlapping bursts. We observe that equations (6) through (8) are valid when h(t) is a bandpass function, but (13) is then meaningless unless we redefine τ_h for a bandpass h(t). Also we note that this definition would be necessary for meaningful use with a burst-counter processor, since it is the bandpass filtered AC signal to wide-band noise power that is significant in that case.

Signal Regimes.- The idealized quantity $SNR_{av\,peak}$ given in equation (13) as $\lambda_j\tau_h$ is at least a useful quantity in defining a classification system of signal regimes for a low-pass

---

*Typical rms values are 0.707 or greater ([22], page 66).

filtered signal. The following definitions of a photon-resolved, a photon-limited, and a Gaussian signal regime have been somewhat arbitrarily* identified:

The signal is photon resolved if $\lambda\tau_h << 1$. In this case the probability of two or more photoelectron events occurring within the response time τ_h is small. Its appearance is that of individual pulses which vary in height due to the randomness of g_i. Photon counting methods are appropriate. The conditional mean value of i(t) is still proportional to $\lambda(t)$, but there is no visible resemblance to $\lambda(t)$. This condition is illustrated by the extreme right hand portion of Figure 2.

For $\lambda\tau_h >> 1$, the signal i(t) is asymptotically a nonstationary Gaussian Process. In this case the first and higher order probability density functions for i(t) at any set of instants $(t_1, t_2, \ldots)$ may be determined immediately by plugging the mean, variance and auto-covariance from the preceding equations into well known Gaussian formulas. Under these same conditions the signal display appears to the eye as a classical signal $m_i(t)$ plus Gaussian noise. This condition is approached by peak of the trace in Figure 2. The major difference between this case and that of classical communications theory problems is that the σ value for the noise is signal (time) and system dependent. Usually, signals in the Gaussian regime are suitable for processing by classical methods (burst counter and/or tracker).

The photon limited regime is that for which $\lambda\tau_h$ is within an order of magnitude of unity. No mathematical simplifications are possible. Visually the signal appears as shown in all but the lowest portions of Figure 2. The upper limits of photon

---

*See Papoulis [10] page 571. No specific limit on the magnitude of $\lambda\tau_h$ is given. We define the photon limited regime as $0.1 < \lambda\tau_h < 10$.

counting techniques and the lower limits of conventional techniques both fall in this range.

As we have illustrated, the signal classification may apply to different portions of the same waveform. We may also use the classification with respect to the peak pedastal value $\lambda_j \tau_h$ to classify signal bursts. Under this type of classification, Figure 2 illustrates a photon-limited burst whose peak average SNR is less than 10. Additional bandpass filtering would increase τ_h and place the central portion of the burst in Figure 2 in the Gaussian regime. This would not be possible with a significantly weaker signal.

Unconditional Statistics

Long time mean, variance, autocovariance.- Equations (6) - (8) include the assumed deterministic classical signal $\lambda(t)$ which is proportional to instantaneous optical power. When we wish later to evaluate the long-time average result which accumulates during a photon counting experiment, it will be necessary to treat $\lambda(t)$ as an ergodic random process with long-time average equal to the unconditioned statistical mean:

$$\langle \lambda(t) \rangle = \lambda \tag{14}$$

We also make use of the autocorrelation of $\lambda(t)$:

$$\langle \lambda(t)\, \lambda(t+\tau) \rangle = R_\lambda(\tau) \tag{15}$$

Now from equation (6) taking the expectation with respect to $\lambda(t)$ gives the average current as

$$\langle i \rangle = e \langle g_i \rangle \langle \lambda \rangle \int_{-\infty}^{\infty} h(t)dt \tag{16}$$

where the integral is unity unless h(t) includes preamplification or attenuation external to the PMT. In order to determine the long time variance σ_i^2 we do not get the correct answer by taking the expectation of $\sigma_i^2(t)$ given by equation (7). Rather, one determines the conditional value of $\langle i^2(t)\rangle$ by adding the square of (6) to (7). The expectation with respect to $\lambda(t)$ follows; finally, the square of equation (16) is subtracted from the unconditional expectation of $i^2(t)$. When all these steps are completed, and similar ones for the unconditional autocovariance, we obtain:

$$\sigma_i^2 = e^2[\langle g_i\rangle^2 \int_{-\infty}^{\infty} R_\lambda(\alpha) f_h(\alpha)d\alpha + \langle g_i^2\rangle\langle\lambda\rangle \int_{-\infty}^{\infty} h^2(\alpha)d\alpha \quad (17)$$

$$- \langle g_i\rangle^2\langle\lambda\rangle^2 (\int_{-\infty}^{\infty} h(\alpha)d\alpha)^2]$$

$$C_{ii}(\tau) = e^2[\langle g_i\rangle^2 R_\lambda(\tau) * f_h(\tau) + \langle g_i^2\rangle\langle\lambda\rangle f_h(\tau) \quad (18)$$

$$- \langle g_i\rangle^2\langle\lambda\rangle^2 (\int_{-\infty}^{\infty} h(\alpha)d\alpha)^2]$$

where

$$f_h(\tau) = \int_{-\infty}^{\infty} h(\alpha)h(\alpha+\tau)d\alpha \quad (19)$$

The second term in the expression for $C_{ii}(\tau)$ vanishes for τ greater than the impulse response time for the PMT and filter combination; the last term is the square of the mean; the first term is the correlation of $\lambda(t)$ smoothed by the correlation of h(t) with itself.

Ideal photon correlation.- An idealized photon correlator counts all photoelectron emission events during successive uniformly spaced clock periods of duration $\Delta\tau$. The number sequence

$\{n_k\}$ which results is algebraically manipulated to yield the summation of terms $n_k n_{k+p}$. In evaluating the expected value of the result of accumulating such a sum we encounter the need to evaluate the quantities $\langle n_k \rangle$ and $\langle n_k + n_{k+p} \rangle$. These expectations may be evaluated using equations (16) - (19) by assuming

$$h(t) = \text{Rect}(t/\Delta\tau) \tag{20}$$

$$g_i = 1/e$$

where Rect(t) was defined in equation (11) and

$$\int h(t)dt = \Delta\tau \tag{21}$$

With these assumptions, i(t) is equal to the number of photoelectron events in the interval $(t - \Delta\tau/2,\ t + \Delta\tau/2)$ and the formulas reduce to

$$\langle i \rangle = \langle n_k \rangle = \langle \lambda \rangle \Delta\tau \tag{22}$$

$$\text{var } n_k = \sigma_i^2 = \langle n_k^2 \rangle - \langle n_k \rangle^2 = \Delta\tau \int_{-\infty}^{\infty} R_\lambda(\alpha)\ \Lambda\left(\frac{\alpha}{\Delta\tau}\right) d\alpha \tag{23}$$

$$+ \langle \lambda \rangle \Delta\tau - \langle \lambda \rangle^2 \Delta\tau^2$$

$$\langle n_k n_{k+p} \rangle = C_{ii}(p\Delta\tau) + \langle i \rangle^2 \tag{24}$$

$$= \Delta\tau R_\lambda(\tau) * \Lambda(\tau/\Delta\tau)\Big|_{\tau = p\Delta\tau,\ p \neq 0}$$

where the correlation integral of equation (19) produces a triangular function, i.e.

$$\int \text{Rect}\left(\frac{\alpha}{\Delta\tau}\right) \text{Rect}\left(\frac{\alpha+\tau}{\Delta\tau}\right) d\alpha = \Delta\tau\, \Lambda(\tau/\Delta\tau) \tag{25}$$

where

$$\Lambda(\tau/\Delta\tau) = 1 - |\tau|/\Delta\tau\ ,\quad |\tau| < \Delta\tau \qquad (26)$$

$$= 0\qquad\qquad ,\quad |\tau| > \Delta\tau$$

We observe that the generally accepted result that the photon correlation is shaped like the correlation of the classical signal is true subject to the jump discontinuity at zero delay and subject to the triangular weighting function which behaves as a low-pass filter with respect to the details of $R_\lambda(\tau)$.

When $\Delta\tau$ is much smaller than a characteristic signal period, then equations (23) and (24) simplify:

$$\langle n_k n_{k+p}\rangle = \Delta\tau^2\, R_\lambda(p\Delta\tau),\ p \neq 0 \qquad (27)$$

$$= \Delta\tau^2\, R_\lambda(0) + \langle\lambda\rangle\Delta\tau,\ p = 0$$

$$\text{var } n_k = \sigma_i^2 = \langle\lambda\rangle\Delta\tau + \Delta\tau^2\,(\langle\lambda^2\rangle - \langle\lambda\rangle^2) \qquad (28)$$

i.e.,

$$\text{var } n_k = \langle n_k\rangle + \Delta\tau^2\ \text{var}\ \lambda \qquad (29)$$

This last result, which we obtain as a special case, has also been given by Bertolotti [21]. It provides a way to measure the variance of the classical signal even with photon resolved signals if a long sequence of n_k values are available.

PHOTON COUNTING PROCESSORS FOR MEAN FLOW AND TURBULENCE INTENSITY

In this section we provide an idealized theoretical basis for the use of photon correlation and a new type of photon

counting technique, "dual-correlate-and-subtract," and show how they may be used for mean-flow and turbulence intensity measurements. Extensions to higher order statistics are discussed in a later section. Error analysis of the processors described in this section is presented in the next section.

Specific Signal Model

The form of equation (5) is quite general. In most practical systems, the function $f(t,\bar{V}_j,\bar{r}_j)$ which describes the optical response with respect to particle position and velocity is complicated when the effects of limiting pinhole apertures and variable duration due to high turbulence are included. For the present we assume a simplified low turbulence model which assumes a burst with perfect contrast and constant shape:

$$\lambda(t) = \lambda_b + \sum \lambda_j f(t - \tau_j)[1 + \cos\, \omega_j(t - \tau_j)] \qquad (30)$$

where λ_j = random burst pedastal amplitude
λ_b = constant background rate,
$f(t)$ = low-pass pulse waveform with peak equal unity,
τ_j = occurrence time for jth burst,
ω_j = radian frequency proportional to one velocity component of the jth particle

We may write equation (30) as the sum of a constant, λ_b, a low-pass process, $\lambda_{\ell p}(t)$, (the pedastals), and a bandpass process $\lambda_{bp}(t)$. Then

$$\lambda(t) = \lambda_b + \lambda_{\ell p}(t) + \lambda_{bp}(t) \qquad (31)$$

We assume that there are several fringes in the probe volume so that the spectra of $\lambda_{\ell p}(t)$ and $\lambda_{bp}(t)$ are non-overlapping. Thus $\lambda_{bp}(t)$ is a zero-mean process, and $\lambda_{\ell p}(t)$ and $\lambda_{bp}(t)$ are uncorrelated. We obtain

$$R_\lambda(\tau) = \langle\lambda(t)\rangle^2 + C_{\lambda\ell p}(\tau) + C_{\lambda bp}(\tau) \qquad (32)$$

We now use the low turbulence assumption and further assume that the scatterers are uniformly dispersed in space so that, R(t), the rate of burst arrivals is a constant R. The results of Appendix A can be applied to derive expressions for the three terms in equation (32), the result is

$$\langle\lambda(t)\rangle = \lambda_b + R\langle\lambda_j\rangle \int_{-\infty}^{\infty} f(t)dt \qquad (33)$$

$$C_{\lambda\ell p}(\tau) = R\langle\lambda_j^2\rangle \int_{-\infty}^{\infty} f(t)\, f(t+\tau)dt \qquad (34)$$

$$C_{\lambda bp}(\tau) = R\langle\lambda_j^2\rangle \frac{1}{2} \langle\cos\,\omega\tau\rangle \int_{-\infty}^{\infty} f(t)f(t+\tau)dt \qquad (35)$$

where the expectation of the $\langle\cos\,\omega\tau\rangle$ term is with respect to the random variable ω_j. The derivation requires that we expand the product of cosines with the sum and difference formula and approximate the integral of the product of a low-pass term and a bandpass term as zero.

We now assume that the turbulence is Gaussian with mean radian frequency ω_m and rms deviation σ_ω. Then by direct application of the definition of expectation we obtain*

$$\langle\cos\,\omega\tau\rangle = \int_{\infty}^{\infty} \frac{1}{\sqrt{2\pi}\,\sigma_\omega} e^{-(\omega-\omega_m)^2/2\sigma_\omega^2} \cos\,\omega\tau\, d\omega \qquad (36)$$

$$= e^{-\sigma_\omega^2\tau^2/2} \cos\,\omega_m\tau$$

*In general $\langle\cos\,\omega\tau\rangle$ is simply related to the statistical characteristic function for the random variable ω_j since this function is defined as a Fourier transform of the probability density function [10].

A simplified expression for the autocorrelation of the classical signal is thus

$$R_\lambda(\tau) = (\lambda_b + R\langle\lambda_j\rangle \int_{-\infty}^{\infty} f(t)dt)^2 \tag{37}$$

$$+ R\langle\lambda_j^2\rangle(1 + \frac{1}{2} e^{-\sigma_\omega^2\tau^2/2} \cos \omega_m\tau)\int_{-\infty}^{\infty} f(t)f(t+\tau)dt$$

This result shows that regardless of the shape of the envelope function f(t), the autocorrelation function has a consinusoidal variation at the mean signal frequency and a Gaussian envelope decay factor due to turbulence intensity.

If we now assume that the classical bursts are Gaussian shaped (TEM_{oo} beams without aperture effects), then we have

$$f(t) = e^{-t^2/\alpha^2} \tag{38}$$

where α is the 1/e half width of the envelope and obtain

$$\int_{-\infty}^{\infty} f(t)dt = \sqrt{\pi}\ \alpha \tag{39}$$

$$\int_{-\infty}^{\infty} f(t)f(t+\tau)dt = \sqrt{\frac{\pi}{2}}\ \alpha e^{-\tau^2/2\alpha^2}$$

The final simplified expressions for the first two moments of $\lambda(t)$ are

$$\langle\lambda\rangle = \langle\lambda(t)\rangle = \lambda_b + R\langle\lambda_j\rangle\sqrt{\pi}\ \alpha \tag{40}$$

$$R_\lambda(\tau) = \langle\lambda\rangle^2 + R\langle\lambda_j^2\rangle\sqrt{\frac{\pi}{2}}\alpha(1 + \frac{1}{2} e^{-\sigma_\omega^2\tau^2/2} \cos \omega_m\tau)e^{-\tau^2/2\alpha^2} \tag{41}$$

where low percent turbulence has been assumed and

λ_b = background count rate,
R = scatterer arrival rate,
λ_j = random pedastal height from jth scatterer,
α = 1/e half burst duration,
σ_ω = rms deviation of radian frequency due to turbulence,
ω_m = mean radian frequency ($\sigma_\omega/\omega_m \ll 1$), and
τ = delay variable of autocorrelation.

The shapes of typical correlation functions for zero turbulence and 10% turbulence are illustrated in Figure 3.

Idealized Photon Correlation of LV Signals

The number n_k is the number of photo-electron emission events in the interval which extends $\pm\Delta\tau/2$ from the instant $k\Delta\tau$. An idealized photon correlator produces and sums delayed products from the uniformly spaced sequence $\{n_k\}$. We assume the total number of products accumulated is N. The accumulator produces a sum $\hat{M}_p$ at the delay value $p\Delta\tau$ given by

$$\hat{M}_p = \sum_{k=1}^{N} n_k n_{k+p} \tag{42}$$

The ideal photon correlator would simultaneously accumulate $N\hat{n}_k$ defined by

$$N\hat{n}_k = \sum_{1}^{N} n_k \tag{43}$$

The unconditional expected value of these sums is obtained from equations (22) and (27) after interchanging expectation and summation as

$$\begin{aligned} \langle\hat{M}_p\rangle &= N\langle n_k n_{k+p}\rangle \\ &= N\Delta\tau^2 R_\lambda(p\Delta\tau), \quad p \neq 0 \\ &= N[\langle\lambda\rangle\Delta\tau + \Delta\tau^2 R_\lambda(0)], \quad p = 0 \end{aligned} \tag{44}$$

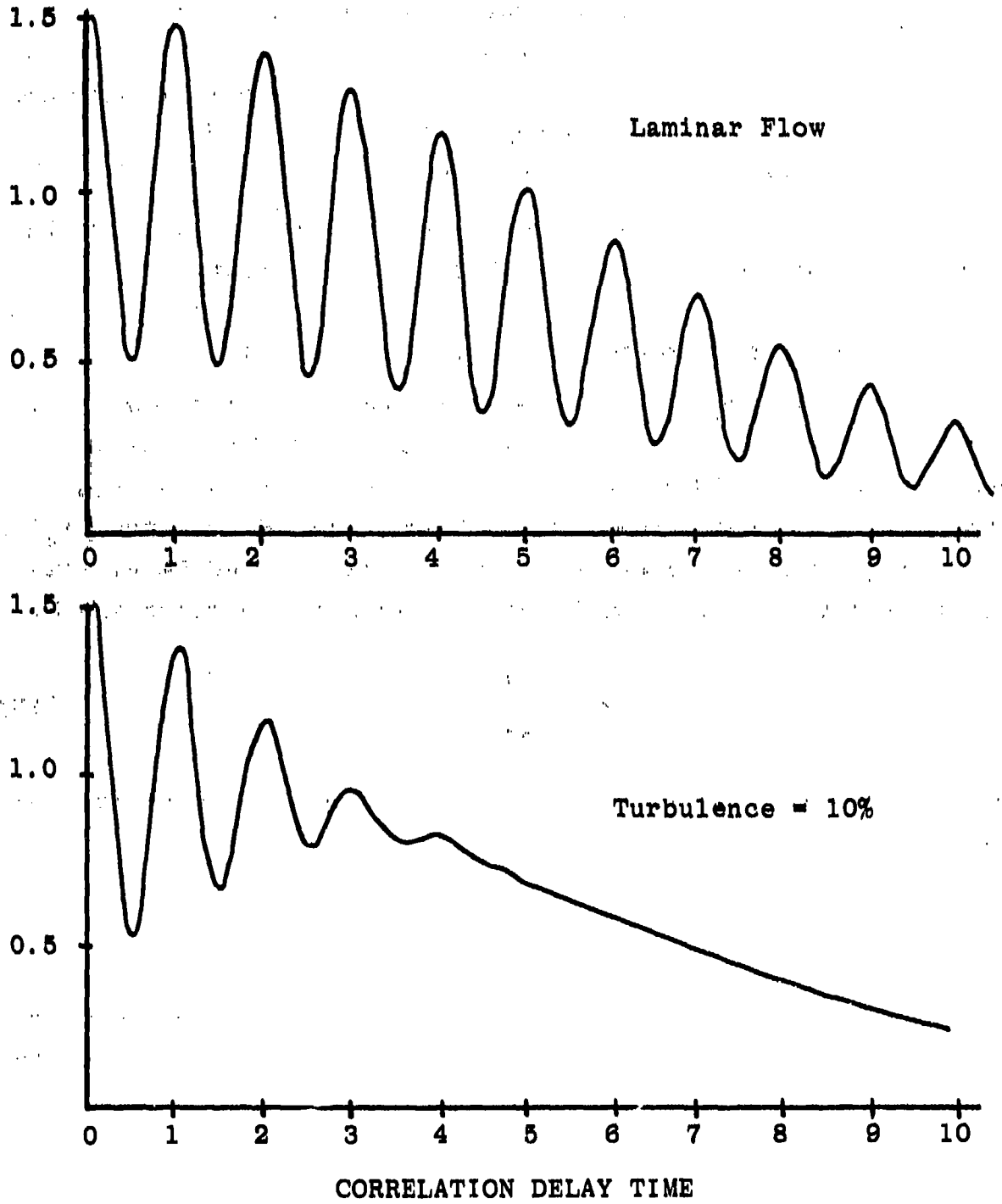

Figure 3. Autocorrelation Functions of Classical Burst Signals.

$$\langle N\hat{n}_k \rangle = N\langle\lambda\rangle\Delta\tau \tag{45}$$

By combining equations (40) - (45), we may obtain an estimator for the autocorrelation of $\lambda(t)$, i.e.,

$$\hat{R}_\lambda(p\Delta\tau) = \frac{\hat{M}_p}{\Delta\tau^2 N} = \frac{1}{\Delta\tau^2 N}\sum_{k=1}^{N} n_k n_{k+p}, \quad p \neq 0 \tag{46}$$

$$\hat{R}_\lambda(p\Delta\tau) = \frac{1}{\Delta\tau^2 N}(\hat{M}_p - N\hat{n}_k), \quad p = 0$$

$$= \frac{1}{\Delta\tau^2 N}\sum_{k=1}^{N} n_k(n_k - 1), \quad p = 0$$

This estimator includes the zero delay value, which is usually omitted, by making use of the separate mean count computation. The same mean count estimate n_k may be used to estimate the long delay level

$$\langle n_k/\Delta\tau\rangle^2 = \langle\lambda(t)\rangle^2 = R_\lambda(\infty) \tag{47}$$

Interpretation of an autocorrelation estimate computed according to equation (46) involves, first, the use of an analytical model such as equation (41); second, a parameter extraction procedure, such as a mean square error minimizing curve fit algorithm; third, a correction for any statistical bias errors; and fourth, a variability error criterion which assures that sufficient data is accumulated. We have provided a procedure and an example model for the first step. The bias and variability errors are discussed in a later section. We have not considered the optimization of the second step although one method is discussed below. Some literature [15,16,17] is beginning to appear, but further effort is needed.

At the Denmark LDA conference in the summer of 1975, Abiss et al. [16] described a "new" interpretation of a photon correlellogram as the Fourier transform of the velocity probability density function. This "breakthrough" allows the measurement of the probability density of the velocity field by digital Fourier transform of the correlation results under the condition that the pedastal and fringe envelope correlations are nearly constant over the range of delays for which the sinusoidal correlation is appreciable. This result is equivalent* to the interpretation of spectrum analyser displays (connected directly to the photo-detector) years ago as the probability density of the velocity field. The restriction is equivalent to requiring many fringes in the probe volume so that the transit-time spectral broadening is small. Our equation (35) shows the relationship between the probability density function of the velocity (frequency) samples and the correlation. The expression $\langle \cos \omega\tau \rangle$ is the cosine Fourier transform of the probability density for ω_j. When there are many fringes in the probe volume the envelope correlation term is a broad pulse which is essentially constant over the extent of $\langle \cos \omega\tau \rangle$. In that case, the transform of the correlation is actually inverting the statistical characteristic function to produce a scaled probability density.

The unfortunate truth remains that in most practical LV problems, the probe volume and spatial frequency of the fringes must be small with the result that we rarely have the luxury of having many fringes in the probe volume. For the realistic case, then, we find the spectrum to be the convolution of the velocity probability density function and the transform of the envelope correlation, and care is required in interpretation.

---

*At least in theory: the photon correlator is much more efficient at low signal levels than any swept frequency spectrum analyser could be.

A Photon Counting Frequency Discriminator

This section describes the basis for a statistical mean frequency discriminator for photon resolved LV signals. We begin with a historical description of the motivating logic which may offer insight to others for more advanced development.

Autocorrelation Frequency Discrimination.- It is well known that the autocorrelation function of a zero-mean narrow-band random process is cosinusoidal with frequency equal to the mean frequency of the narrow-band process and envelope which is the autocorrelation of the amplitude and phase envelope of the process. For example, if the two-sided power $S_x(f)$ of a random process $x(t)$ is

$$S_x(f) = A(f - f_m) + A(f + f_m) \tag{48}$$

Where $A(f)$ is an even pulse-shaped function and f_m is a center frequency much greater than the frequency width of $A(f)$, then

$$R_x(\tau) = 2R_a(\tau) \cos 2\pi f_m \tau \tag{49}$$

Where $A(f)$ is the Fourier transform of $R_a(\tau)$. Now we note that for small perturbations of the argument $2\pi\tau f_m$ about the point

$$\tau = 3/4\ f_m \tag{50}$$

the value of $R_x(\tau)$ varies in proportion to the perturbation of either τ or f_m. Thus, if τ is selected to satisfy equation (50), then the statistical autocorrelation function would serve instantaneously* as a frequency discriminator for small deviations

*This is significant in later sections even though the statistical autocorrelation function cannot be experimentally observed.

of f_m. If the random process were ergodic, then the same results would apply to time-average autocorrelations when the averaging time was long compared with the coherence time of the process. These principles may be extended to a random process which is the sum of a narrow-band process and a low-pass process by first filtering the process with a high-pass filter to remove the non-zero mean low-pass process.

Application to photon resolved signals.- In the case of photon-resolved LV signals, the classical signal random process is not necessarily recoverable from the sparse single photon events, but we have already shown that the autocorrelation function may be approximated by the expected value of a photon correlation operation on the photon events. The original concept was thus to devise a high-pass digital filter which would be applied to the count sequence $\{n_k\}$ to remove the effects of background light and low-pass pedastal from the statistical average $\langle n_k \rangle$ while leaving the bandpass information signal information. This filter would be followed by a digital correlation (delayed product summation) at the delay value given by equation (50). Since the digital electronics had to be very fast, only simple digital filters could be considered. The simplest one that we thought of was to delay the sequence $\{n_k\}$ by one-half period of the signal and subtract. This operation cancels the low-frequency portions of the expected value of n_k and adds the sinusoidal portions in phase. Such a delay and subtract filter would produce

$$m_k' = n_k - n_{k-q} \tag{51}$$

Where the counting interval $\Delta\tau$ must be adjusted to satisfy

$$q\Delta\tau = 1/(2f_m) \tag{52}$$

with q an even integer. After this was done one would accumulate lag products of m_k with delay $p\Delta\tau$ equal to three quarters of a signal period $p = 3q/2$. This approach leads one to form the summation $\hat{M}'_{pq}$ given by

$$\hat{M}'_{pq} = \sum_{k=1}^{N} - n_{k-p}n_{k-q} + 2n_k n_{k-p} - n_k n_{k-p-q} \qquad (53)$$

The previous results for photon correlation are applicable for the determination of the expected value of the quantity $\hat{M}'_{pq}$. The details are omitted here and included for the simpler dual-correlate approach described below, but Figure 4 is a simplified discriminator characteristic for the expected value of the result. It is provided for comparison with Figure 5 which is described in detail below.

After all of the above reasoning, it occurred to us that another approach (we thought) consisted of performing the delay and subtract filtering operation on the correlation estimate after it was made rather than on the high-speed signal sequence $\{n_k\}$. Reference to Figure 3 shows that a one-half-period shift and subtract of the typical LV correlation will approximately cancel the low-pass portion of the autocorrelation. The results of this approach provide an approximate discriminator response as shown in Figure 5 with less high-speed data arithmetic required. This "dual correlate and subtract" approach also leads to larger frequency range for the discriminator function, and thus has been chosen for development. Hindsight has now shown us that by algebraic rearrangement this approach is most economically implemented with high-speed delay and subtract filter prior to multiplication. This technique may be shown to be just another implementation of the original filter and correlate concept.

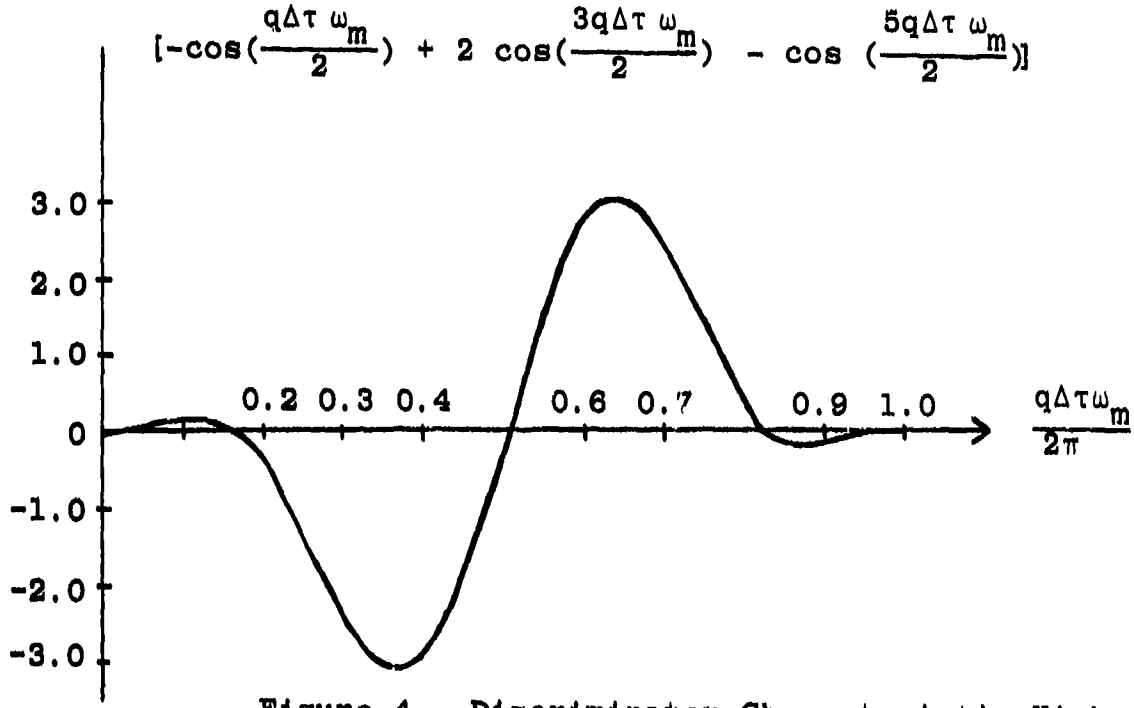

Figure 4. Discriminntor Characteristic High Pass and Correlate Mode.

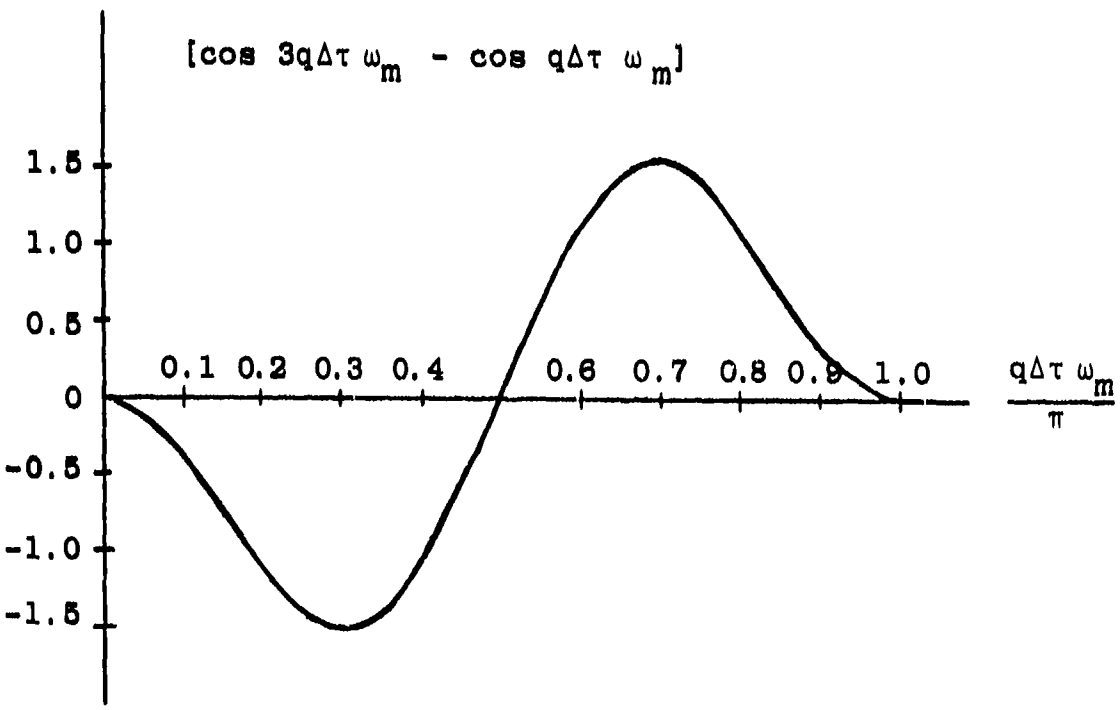

Figure 5. Discriminator Characteristic for Dual Correlate Approach.

Dual correlate and subtract.- We will let the quantity $\hat{M}_{pq}$ be defined as follows

$$\hat{M}_{pq} = \sum_{k=1}^{N} m_k \tag{54}$$

$$= \left(\sum_{k=1}^{N} n_k n_{k-p} \right) - \left(\sum_{k=1}^{N} n_k n_{k-q} \right)$$

where

$$m_k = n_k (n_{k-p} - n_{k-q}) \tag{55}$$

It is straight forward to show that, except for a few end terms, $\hat{M}_{pq}$ is mathematically identical to the quantity $\hat{M}_p - \hat{M}_q$ where $\hat{M}_p$ and $\hat{M}_q$ are defined by equation (42). It is for this reason that we will lable the approach as the "Dual Correlate and Subtract" technique even though the delay values are negative instead of positive.* We now demonstrate that the expected value of $\hat{M}_{pq}$ behaves as a frequency discriminator as illustrated in Figure 5 under conditions which we will identify. The adjustment of the system clock period $\Delta\tau$ leads to a null in the expected accumulator value. Measurement of $\Delta\tau$ provides a direct measure of the mean signal frequency as we shall now show with our simplified signal models.

From equation (44) we obtain the expected value of the estimator as

$$\langle \hat{M}_{pq} \rangle = N\Delta\tau^2 [R_\lambda(p\Delta\tau) - R_\lambda(q\Delta\tau)] \tag{56}$$

The complete expression is obtained for our simplified signal

---

*The negative delay implementation was more suitable for the hardware design.

model by using equation (41) in its entirety. Here we assume that $p\Delta\tau$ and $q\Delta\tau$ are both small compared with α so that the pedastal terms cancel as well as the steady term. This leaves

$$\langle \hat{M}_{pq} \rangle = N\Delta\tau^2 R \langle \lambda_j^2 \rangle \frac{1}{2} \sqrt{\frac{\pi}{2}} \alpha \, . \tag{57}$$

$$\cdot \left[e^{-\frac{1}{2}\left(\frac{1}{\alpha^2} + \sigma_\omega^2\right)(p\Delta\tau)^2} \cos \omega_m p\Delta\tau - e^{-\frac{1}{2}\left(\frac{1}{\alpha^2} + \sigma_\omega^2\right)(q\Delta\tau)^2} \cos \omega_m q\Delta\tau \right] .$$

Now we require that

$$p = 3q \tag{58}$$

and observe the behavior of equation (57) near the values of $\Delta\tau$ specified by letting $q\Delta\tau$ be one quarter of the signal period where both cosine terms will vanish.

$$q\Delta\tau = 2\pi/4\omega_m = T_m/4 \tag{59}$$

The shape of the term in braces is plotted in Figure 5 under the assumption of many fringes in the probe volume (α large) and low turbulence (σ_ω small). Thus the quantity plotted is simply

$$[\cos 3q\Delta\tau \ \omega_m - \cos q\Delta\tau \ \omega_m] \tag{60}$$

Figure 5 illustrates the expected behavior of the accumulator sum for changes in the mean signal frequency ω_m. If the system clock frequency is changed to change $\Delta\tau$, then the response is the product of $\Delta\tau^2$ and the curve shown in the figure. The shape of the curve is affected but the zero crossing locations are not.

Selection of delay constants.- The theory does not uniquely specify the relationship of $\Delta\tau$ (the above system clock period) to T_m the signal period because q is not specified. For a given value of signal period, T_m, the largest possible value of $\Delta\tau$ for an acceptable null is when $q = 1$ and $\Delta\tau = T_m/4$. This produces the least variability error (as we will show) and the most bias error due to time smear (the triangular weighting function in equation (24). The value $q = 1$ also allows the highest signal frequencies to be measured for a given maximum system clock frequency. The bias errors can be reduced at the expense of increased variability error and reduced maximum signal frequency by using $q = 2$, $\Delta\tau = T_m/8$. In order to facilitate experimental research, our design for a research instrument allows selection of p and q over a wide range.

STATISTICAL ERROR ANALYSIS

Introduction

The two principle types of error which arise in statistical measurements are bias error and variability error. Bias error is a term which refers to the difference between the statistical expectation of the measurement system output and the desired average value being measured. The variability error is the rms value of the random deviation of a specific experimental result from the statistically expected value. For ergodic random processes, the variability error converges to zero in the limit of infinitely long data collection time; but it converges to an acceptable level (which must be defined in the measurement objectives) within a finite measurement time. The bias error cannot be removed by further averaging but it can often be removed by analytical compensation or by experimental calibration when it is small compared with the desired

quantity. In general, analysis of both types of errors is required in any statistical measurement.

There are three different methods for evaluation of the statistical errors of a measurement system; these are: analysis, simulation, and experiment. Appendix A provides theory for the higher order moments of inhomogeneous Poisson processes which we have expanded for application to the demonstration of concepts in the previous sections and analysis of errors in this section. The study of the theory of Poisson processes has also provided the concepts necessary for digital simulation of the LV signals and their detection by photon counting systems. The concepts and a FORTRAN computer program which we have developed for this simulation are provided in Appendix B. The simulation provides a method of investigating such nonlinear effects as processor dead time and counter saturation which we have not yet been able to do with analysis.

Bias Errors

The sources of bias errors which have been studied in the measurement of mean flow are as follows: fringe number, turbulence intensity, time smear, and dead time.

Fringe number and turbulence intensity.- When the number of fringes N in the probe volume is small, subtraction* of $R_\lambda(\tau = 3T_m/4) - R_\lambda(\tau = T_m/4)$ is slightly negative instead of zero. The error becomes significant only for small values of N_f. The signal frequency estimate using the zero criterion will be too small. We have computed the error in percent in the following manner.

Let $R_\lambda(3q\Delta\tau) - R_\lambda(q\Delta\tau) \triangleq \psi(q\Delta\tau)$. For large number of

*This error pertains to the dual correlate and subtract technique.

fringes ($N \to \infty$) then $\psi(q\Delta\tau) = 0$ when $\Delta\tau = \frac{T_m}{4}$ where T_m is the mean signal period. When $N < \infty$, then

$$R_\lambda(3T_m/4) - R_\lambda(T_m/4) = \Delta\varepsilon = \psi(\Delta\tau = T_m/4) \leq 0 \quad (61)$$

The correct value of $q\Delta\tau$ for $\psi(q\Delta\tau) = 0$ is $q\hat{\Delta\tau} \cong T_m/4 + \frac{\Delta\varepsilon}{\psi'(T_m/4)}$ and the fractional error ε in accepting $\psi(q\Delta\tau) = 0$ as indication that $q\Delta\tau = T_m/4$ is approximately

$$\varepsilon = \frac{4\psi(T_m/4)}{T_m\psi'(T_m/4)} \quad (62)$$

We have evaluated ε for various levels of ρ = rms turbulence/mean velocity and for N_f = number of static optical fringes in $1/e^2$ signal width.

The result of the parametric computations are presented in two forms in Figures 6 and 7. From the results we conclude that the bias error is not very sensitive to turbulence intensity at the levels shown. A first order correction independent of turbulence is thus possible. A second order correction is possible with only very imprecise estimates of turbulence intensity.

Time smear error and correction techniques.- The photons represented by the count n_k at time $k\Delta\tau$ were in fact smeared in occurrence time over the range $[(k - 1/2)\Delta\tau, (k + 1/2)\Delta\tau]$. The effect of this is usually neglected by assuming $\Delta\tau$ is small compared with any significant variations in the classical signal. This is never true in the most difficult experimental cases where the electronic speed limitations force $\Delta\tau$ to be an appreciable function of the signal period T_m. The result provided in equation (24) for photon correlation included the time

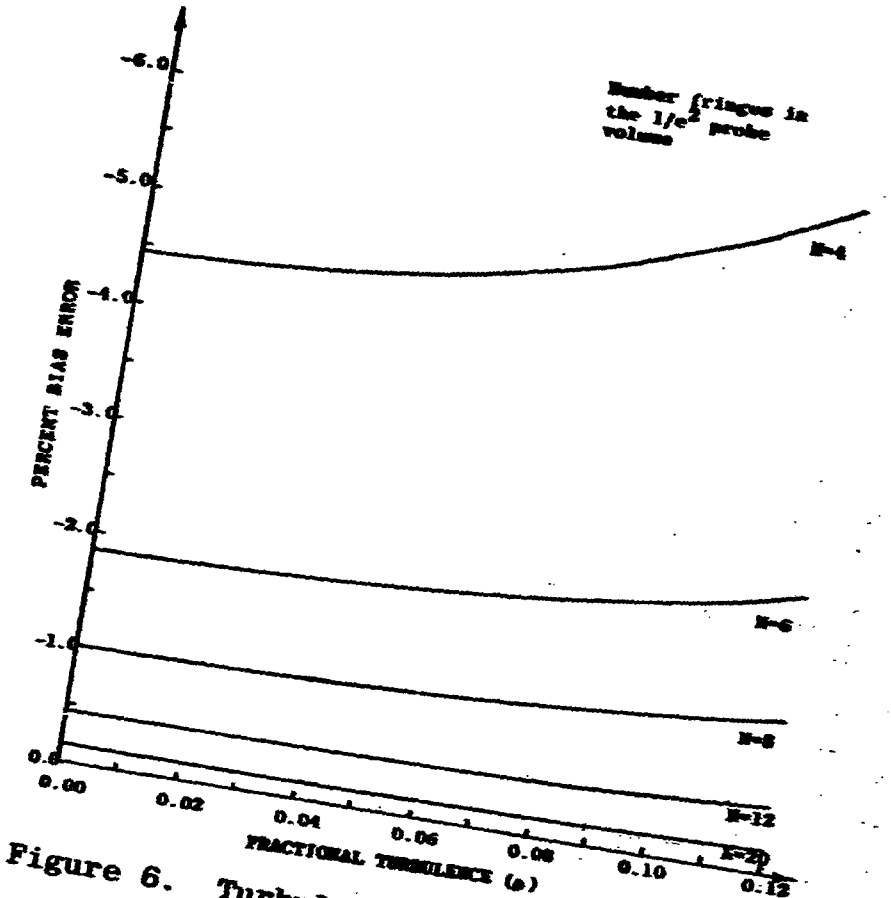

Figure 6. Turbulence Intensity Mean Bias.

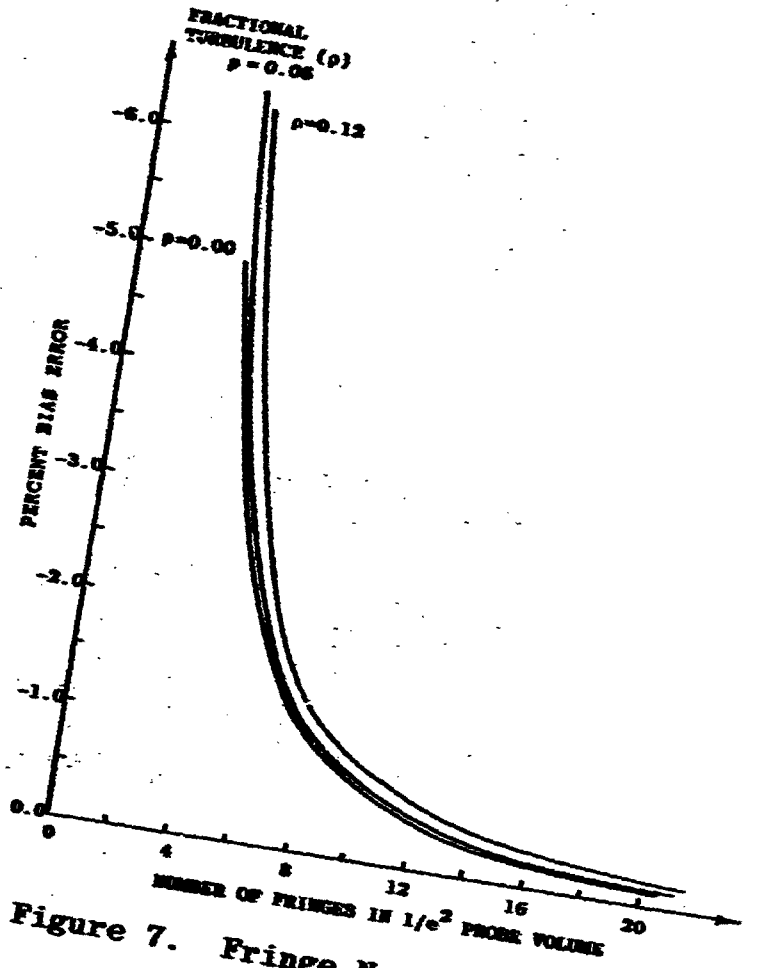

Figure 7. Fringe Number Mean Bias.

smear effect in the triangular function Λ which convolves with the autocorrelation of the classical signal. After equation (26) the triangular function was treated as a delta function, i.e., in the limit of small $\Delta\tau$,

$$\frac{1}{\Delta\tau}\,\Lambda(\tau/\Delta\tau) \to \delta(\tau) \tag{63}$$

and equation (27) results from the convolution.

Now, if we do not make the limit assumption,* we note that the effects of the triangle function are easily displayed in the frequency domain: From Bracewell [24] we have the relationship .

$$\int_{\infty}^{\infty} \frac{1}{\Delta\tau}\,\Lambda(\tau/\Delta\tau)e^{-j2\pi f} = \text{sinc}^2\,(f\Delta\tau) \tag{64}$$

where

$$\text{sinc}\,(f\Delta\tau) = \frac{\sin \pi f\Delta\tau}{\pi f\Delta\tau} \tag{65}$$

This Fourier transform relationship is illustrated in Figure 8. The convolution theorem of Fourier transform theory assures us that in the frequency domain, the effect of the convolution in equation (24) is a product. In other words, the frequency spectrum associated with the signal correlation by Fourier transform is attenuated by a low-pass filter whose form is sinc $(f\Delta\tau)$. This function is plotted in Figure 8c. As the figure shows, there is little attenuation when $f_m\Delta\tau = \Delta\tau/T_m = 1/16$, i.e., when the clock period is 1/16 of the signal period. For

*The effect of time discretization is a $\text{sinc}^2(f)$ type of low-pass filter. This is similar to a result in our previous work of determing turbulence power spectra from randomly tried samples [23].

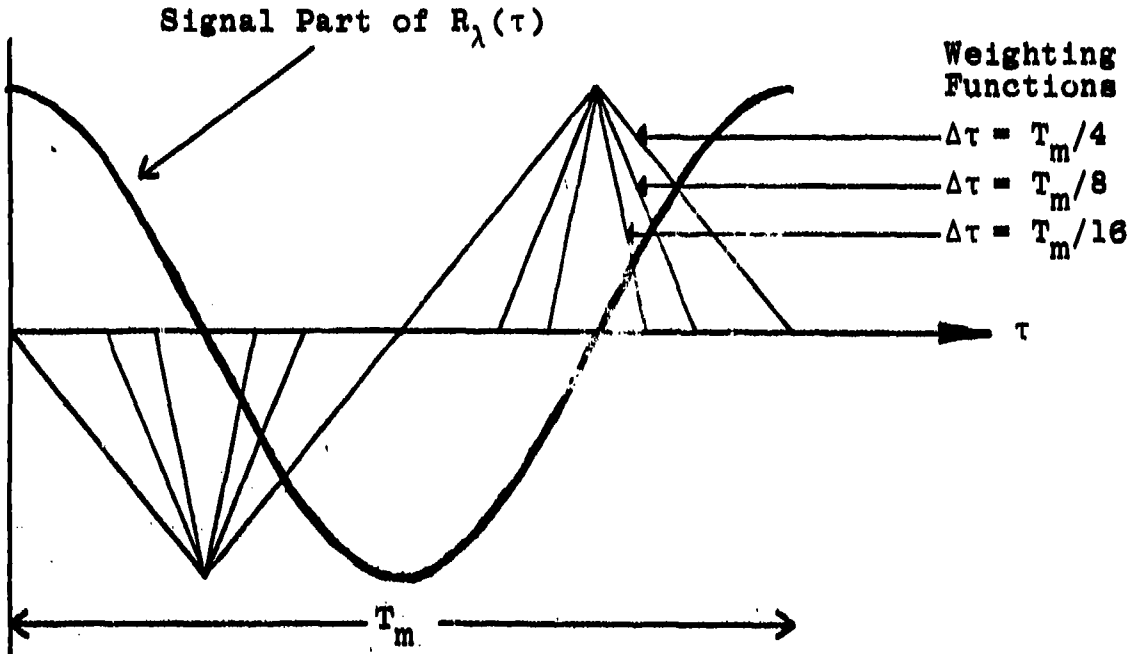

(a) Triangular Weighting Functions corresponding to choices for $\Delta\tau$ relative to mean signal period. (illustrated at delay locations for Dual Correlate Approach)

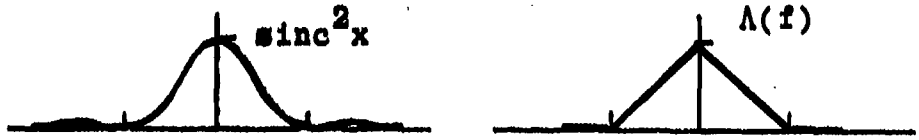

(b) Fourier transform relationship of Λ and sinc^2 function

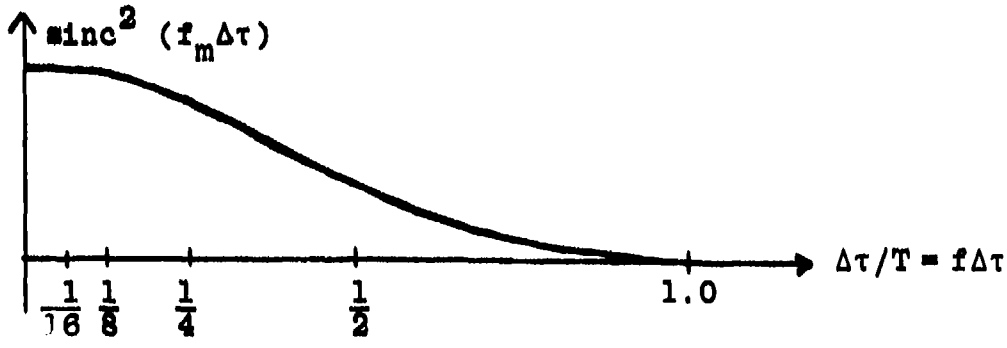

(c) Low Pass Filter effect of $\Delta\tau$ selection.

Figure 8. Time Smear Effects of Finite $\Delta\tau$.

very low turbulence and a large number of fringes N_f, the signal spectrum would be small in width and $\Delta\tau$ could be made as large as $T_m/2$.* However, for values of $\Delta\tau > T_m/8$ we see that a correction of the velocity probability density function could be useful for all but very small turbulence levels. Such a correction would be effected by multiplying the transform of the correlation estimate by $1/\text{sinc}^2\ (\Delta\tau f)$ prior to final data interpretation.

Dead time effects.- No physically realizable photodetector and electronic counter combination can be constructed without some dead time; i.e., a period of time following a threshold crossing by the analog photodetector voltage waveform during which no additional crossing events will be counted. This dead time is typically 10 nsec for commercial photon discriminator circuits at the time of this writing. There is no fundamental reason why this cannot be reduced to less than 5nsec with the fastest photomultiplier tubes and counting circuits now available. We will also distinguish two other types of counting dead time. The first of these is "pulse pile up" in which the photodetector analog waveform remains above the threshold level due to there being more than one photoelectron event within the pulse response time of the photo detector. There is also a brief interval during the periodic counting interval during which the counter is being reset and is not available. This is true even when two counters are used alternately, since a small guard interval is required to keep both counters from counting the same event. Practical dead intervals τ_r may be on the order of 2nsec or less.

---

*This limit could be actually exceeded because the sampling theorem really refers to bandwidth, not maximum frequency; however, the attenuation would then be severe.

The counter dead interval τ_r will be considered first since it is the simplest. To first order it can be neglected, but correction in the formulas is simple. It is only necessary to replace $\Delta\tau$ by $\Delta\tau-\tau_r$ in the theoretical formulas where the $\Delta\tau$ refers to the counting width. The amount of delay remains equal to some integer multiple of $\Delta\tau$. As a simple example the mean value of n_k becomes $\langle\lambda(t)\rangle(\Delta\tau-\tau_r)$ instead of $\langle\lambda(t)\rangle\Delta\tau$.

The effects of pulse pile up are least known for the photon-limited signal cases. For higher photon rates the PMT analog waveform will generally remain above the photon counting threshold and so produce no counting effects. The pulse pile up effects can be studied with the present signal simulation program (see Appendix B) when a more complete processor simulation subroutine is completed in the future. At present the photon processor simulation is idealized so that discretized photoelectron event times are used directly without synthesis of the PMT anode waveform and a threshold crossing circuit model.

The effects of discriminator dead-time effects have been presented analytically by Jakeman* for the case of Gaussian optical electric field statistics. We have not yet extended the theory to the single-particle LV signal situation (non-Gaussian field statistics) and can offer no improvement analytically here over Jakeman's results. However, we dispute Jakeman's conclusion* that in practice dead time errors are not a serious limitation of photon correlation. The seriousness of the effect is demonstrated below using the computer simulation program provided in Appendix B.

We have simulated a wind tunnel instrumentation example with the constants given in Table 1. The results are

---

*Page 116, [12].

Theory Symbol	Program Name	Value	Description
T	TTOT	10^{-3}sec	Total time limit
	MNTOT	3×10^{3}	Photoelectron limit
Σn_k	KMAX	480	Number of Δt's per burst
$\langle \lambda_j \rangle$	AFAC	10^{7}/sec	Mean peak pedastal rate
	HIGH	10	Max λ_j = High $\cdot \langle \lambda_j \rangle$
	LOW	0.1	Min λ_j = Low $\cdot \langle \lambda_j \rangle$
	IR2	4	λ_j = AFAC (not random)
1/R	TB	5×10^{-6}	Mean time between bursts
	THEORY	TRUE	Logical: Selects ideal processor
	MAXC	10^{3}	Maximum count of processor (high to avoid limitation here)
$\alpha\sqrt{2}$	D	8×10^{-7}sec	$1/e^2$ half width of bursts
	CON	3	D CON = Total burst width
	AME	1.0	Burst modulation index
f_m	FO	6.25×10^{6}Hz	Signal frequency
$\Delta\tau/\Delta t$	ITAU	4	Ratio of processor resolution to simulation resolution
	IP	20	Maximum correlation delay
	WAVE	TRUE	Logical: True=Bursts present
$\lambda_b = 0$	CONST	FALSE	Background: True=λ_b present
$\tau_d/\Delta t$	DEAD	0,1,2,3,4	Dead time in Δt units
Δt	DT	5 nsec	Simulation resolution interval
$\Delta\tau$	DT*ITAU	20 nsec	Processor resolution interval
	ONE	FALSE	Logical: Time=Dual Correlate

TABLE 1. PARAMETER SELECTIONS FOR DEAD TIME SIMULATION.

plotted in Figure 9. For comparison, the figure also shows the theoretical expected value of the accumulator sums as predicted by the following equations. We use the values in Table 1 with equations (40), (41) and (44) to obtain the mean level $\langle\lambda(t)\rangle$ as

$$\langle\lambda\rangle = 2.005 \times 10^{6} \text{ photoelectrons/sec} \qquad (66)$$

$$\langle\hat{M}_p\rangle = 80.4 + 283.6\ (1 + \tfrac{1}{2}\cos 2\pi f_m \tau) e^{-\frac{\tau^2}{2(5.66 \times 10^{-7})^2}} \qquad (67)$$

where

$$\tau = (p\Delta\tau) = p(20 \times 10^{-9} \text{ sec})$$

$$f_m = 6.25 \times 10^{6} \text{ Hz}$$

From Figure 9 it is clear that for dead times which are an appreciable fraction of the clock interval, there will be distortion of the correlation functions. This does not appear to be a problem for $\Delta\tau = Tm/8$ except at the first delay valve and a general amplitude reduction but further study is needed. The dead time effect is seen to seriously affect the first delay; this will seriously affect the dual correlate approach if $\Delta\tau = Tm/4$.

Variability Error

In this section we derive formulas for the fractional rms error of a mean flow measurement with a dual correlate and subtract system in terms of the mean photon rate and the system response (integration) time. We assume that the accumulator sum is zero after summing for total time T. This implies that the clock frequency is in error by an amount required to cancel a random (finite time) variability error in the accumulator sum. These compensating errors are assumed small so that a perturbation may be used.

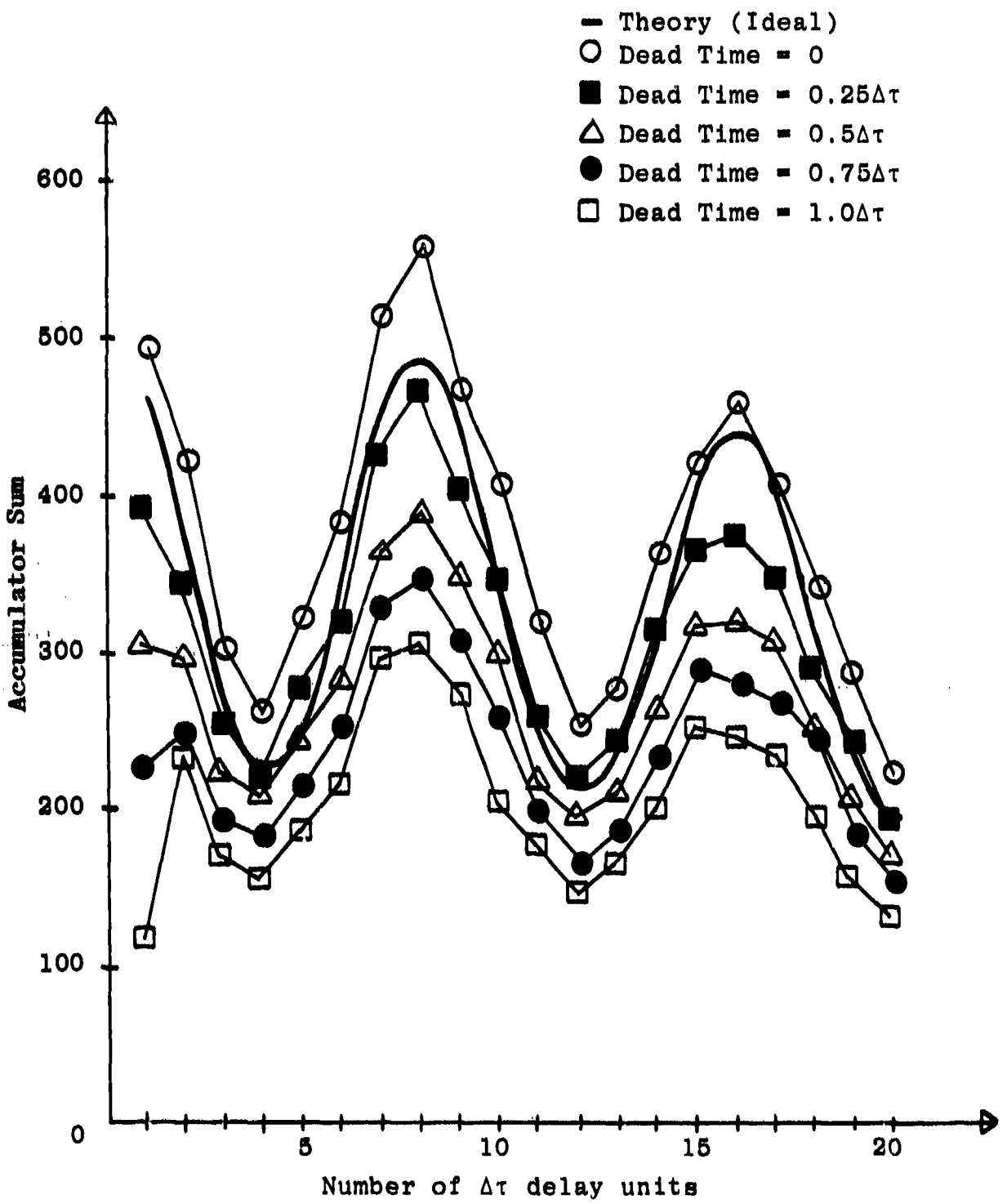

Figure 9. Simulated Effects of Dead Time on Photon Correlation.

An error ε_A in the accumulator sum is equivalent to an error ε_T in the estimation of one quarter of the mean signal obtained by dividing by the slope of the discriminator function $A(\tau)$

$$\varepsilon_T = \varepsilon_A / A'(T_m/4) \tag{68}$$

where $A(\tau)$ is an abbreviation for $\langle \hat{M}_{pq} \rangle$ given earlier in equation (56) and (57). The fractional error ε in estimating the period T_m is thus

$$\varepsilon = \frac{\varepsilon_A / A'(T_m/4)}{T_m/4} = \frac{4\varepsilon_A}{T_m A'(T_m/4)} \tag{69}$$

This is the same form as equation (62) with the only difference being the type of error. We proceed by obtaining a simplified expression for $A(T_m/4)$ by neglecting the Gaussian exponentials in equation (57). Evaluation of the derivatives gives

$$A'(T_m/4) = N\Delta\tau^2 R \langle \lambda_j^2 \rangle \frac{4\pi}{T_m} \sqrt{\frac{\pi}{2}}\, \alpha \tag{70}$$

The quantity ε_A is the rms deviation of the accumulator value M_{pq} after data collection time T. The evaluation of this quantity is discussed in Appendix C and the result for cases where the steady background light is larger than the signal is obtained.* For this case we have

$$\varepsilon_A = \sqrt{2N}\, \lambda_b \Delta\tau \tag{71}$$

When these results are combined we have the fractional error in the velocity estimate given by

---

*This is simpler to evaluate than the low background case and gives a bound on the time required to produce a given error in cases where the background is less.

$$\varepsilon = \frac{2\lambda_b}{\alpha\sqrt{T\Delta\tau}\ R\langle\lambda_j^2\rangle\pi\sqrt{\pi}} \qquad (72)$$

where

λ_b = background photoelectron rate >> signal rate

α = burst 1/e half width

$\langle\lambda_j^2\rangle$ = mean square peak pedastal burst amplitude (photoelectron rate)

R = rate of occurrence of bursts

T = total time = $N\Delta\tau$

ADVANCED PHOTON PROCESSOR FOR TURBULENCE TIME STATISTICS

Introduction

In this section we propose and analyse a photon-processing scheme for estimation of the temporal autocorrelation of the time varying velocity fluctuations. Part of the basis for this is the fact that the frequency discriminator characteristic of Figure 5 applies not only to the long time average of the dual correlate and subtract sum $\hat{M}_{pq}$ but also instantaneously in a conditional statistical sense. We may therefore tune $\Delta\tau$ to the value which centers the long-term average at the zero of the frequency characteristic and then obtain short periodically occurring accumulations of $\hat{M}_{pq}$ whose conditional expected values follow the velocity deviation. Even when the photoelectron rate is small, the correlation of the velocity fluctuations may then be obtained by conventional digital correlation of the sequence of short time $\hat{M}_{pq}$'s.

We define here ΔT as a period greater than $\Delta\tau$, the processor counting interval, and less than the significant times of change of the turbulent fluctuations. The quantity $\hat{M}_{pqn}$ is a sum over the interval $[(n-1)\Delta T < t < n\Delta T]$ of m_k defined in equation (55) as

$$m_k = n_k(n_{k-p} - n_{k-q}); \tag{73}$$

i.e., $\hat{M}_{pqn} = \hat{M}_{pq}$ over the nth ΔT interval. We will consider an autocorrelation estimate of the $\hat{M}_{pqn}$ sequence:

$$\hat{R}_s(i\Delta T) = \frac{1}{N_t - i} \sum_{n=1}^{N_t - i} \hat{M}_{pqn}\hat{M}_{pq(n+i)} \tag{74}$$

We will show that the expected value of this sequence contains the shape of the turbulence autocorrelation function under certain conditions. Further it appears that the magnitude of the turbulence intensity may be obtained by a normalization procedure which will be discussed.

Spectral Analysis of Randomly Sampled Signals

Continuous Functions.- In our previous development [23] we showed that correlations and frequency power spectra can be obtained from randomly timed discrete samples of a velocity component u(t) where the sampling function z(t) is a uniform Poisson impulse process. The same principles may be generalized to the present more complicated data processing problem. First, let us assume that a continuous signal s(t) is available such that

$$s(t) = x(t)\rho(t) \tag{75}$$

$$\rho(t) = u(t)/\bar{U} \tag{76}$$

where u(t) is a zero-mean time-varying velocity component deviation from the mean component $\bar{U}$ and the random process x(t) is a filtered Poisson shot noise process (see Appendix A) statistically independent of u(t):

$$x(t) = \sum_{j=\infty}^{\infty} b_j f(t - \tau_j) \tag{77}$$

Here f(t) is a low-pass impulse response function, the τ_j's are random occurrence times which obey a stationary Poisson law, and the b_j's are equally-distributed statistically-independent random amplitude variables. The functions are illustrated in Figure 10. From the properties of Poisson processes we know that if f(t) is a positive function, then $R_x(\tau) = \langle x(t)x(t+\tau)\rangle$ is a positive function and, making use of the independence assumption

$$R_\rho(\tau) = \langle \rho(t)\rho(t+\tau)\rangle = R_s(\tau)/R_x(\tau) \tag{78}$$

We observe that the zero value of $R_\rho(\tau)$ is the normalized mean-square turbulence intensity $\langle \rho^2 \rangle$. Figure 10 illustrates the fact that when the duration of the pedastal correlation is small compared with the duration of the velocity correlation, the value $\langle \rho^2 \rangle$ may be obtained approximately from $R_\rho(\tau)$ where τ is small but greater than the pedastal duration. If the turbulence intensity is obtained in some other manner, we may theoretically obtain the shape of $R_\rho(\tau)$ even without obtaining $R_x(\tau)$, except in the vicinity of $\tau = 0$, since $R_x(\tau)$ = constant elsewhere.

We may extend the above reasoning to the situation where two sets of processes are available

$$s_1(t) = x_1(t)\rho_1(\bar{r}_1, t) \tag{79}$$

$$s_2(t) = x_2(t)\rho_2(\bar{r}_2, t)$$

So long as x_1 and x_2 are independent of ρ_1 and ρ_2, then

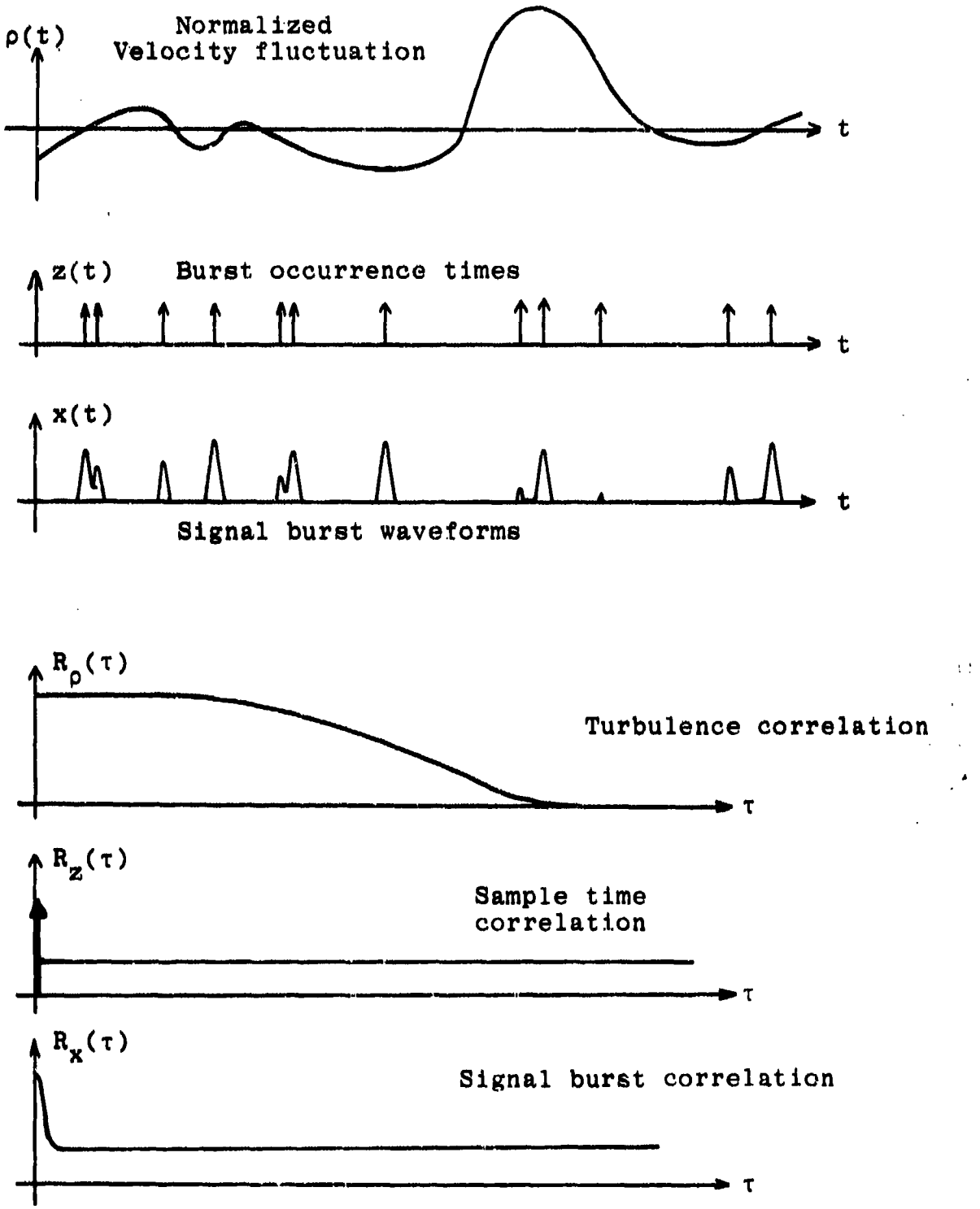

Figure 10. Random Sampling Waveforms and Correlation Functions.

$$R_{s12}(\tau) = \langle s_1(t)s_2(t+\tau)\rangle \tag{80}$$

$$= \langle x_1(t)x_2(t+\tau)\rangle\langle \rho_1(\bar{r}_1,t)\rho(\bar{r}_2,t+\tau)\rangle$$

$$= R_{x12}(\tau)R_{\rho 12}(\tau)$$

and the cross correlation $R_{\rho 12}(\tau)$ may be obtained by division

$$R_{\rho 12}(\tau) = R_{s12}(\tau)/R_{x12}(\tau) \tag{81}$$

The frequency power spectra are Fourier transforms of the correlation functions.

Sampled Data Estimates.- In the preceding, we assumed s(t) and x(t) were continuous and computed statistical correlation functions. We now suppose that real-valued discrete samples S_n and X_n of s(t) and x(t) are taken at uniform intervals ΔT which are small compared with the duration of the random sampling pulse f(t) and correlation time of $\rho(t)$. We may form discrete estimates of $R_s(\tau)$ and $R_x(\tau)$ at $\tau = i\Delta T$ by computing a finite time average, for example

$$\hat{R}_s(i\Delta T) = \frac{1}{N_t - i}\sum_{n=1}^{N_t - i} S_n S_{n+i} \tag{82}$$

where $N_t\Delta T$ is the accumulation time T and the expected value is

$$\langle \hat{R}_s(i\Delta T)\rangle = R_s(\tau = i\Delta T) \tag{83}$$

If such estimates are formed for R_x and R_s, then we may form an estimate for $R_\rho(\tau)$ by division:

$$\hat{R}_\rho(i\Delta T) \triangleq \hat{R}_s(i\Delta T)/\hat{R}_x(i\Delta T) \tag{84}$$

This procedure does not insure that $\langle R_\rho(i\Delta T)\rangle$ is an unbiased estimate but it becomes one in the limit of sufficiently long accumulation time when the numerator and denominator converge to their respective expected values.

Conditional Expectation Again.- The problem is still more complicated. Because we do not have the classical optical signal $\lambda(t)$ available for direct observation, we cannot form $x(t)$ and $s(t)$, or even X_n and S_n. We will process the fast photon-counting sequence n_k to obtain discrete-valued sequences M_{xn} and M_{sn} whose conditional expected values given $\lambda(t)$ are proportional to X_n and S_n.

We thus have an estimate $\hat{R}_s(i\Delta T)$ defined not by equation (82), but by

$$C^2\hat{R}_s(i\Delta T) = \frac{1}{N_t - i}\sum_{n=1}^{N_t-i} M_{sn}M_{s(n+i)} \qquad (85)$$

The expected value of the estimate is

$$\langle M_{sn}M_{s(n+i)}\rangle = \langle\langle M_{sn}|\lambda(t)\rangle\langle M_{s(n+i)}|\lambda(t)\rangle\rangle \qquad (86)$$

$$= C^2\langle S_j S_{j+i}\rangle$$

$$= C^2 R_s\,(i\Delta T)$$

where C^2 is the proportionality constant. This result depends on the fact that given $\lambda(t)$ the discrete random variables M_{sn} and $M_{s(n+i)}$ formed from non overlapping portions of the sequence n_k are conditionally independent. This follows from the fact that n_k is Poisson counting process.

In equation (86) the notation $\langle x|\lambda\rangle$ denotes "expected value of x given λ" and we made use of the fact that the unconditional expectation may be obtained in two steps: first, with respect to x given λ; then with respect to λ.

Application to Photon Processing of Turbulence Correlation

It remains for us to identify measurable quantities with the properties attributed to M_{sn} and M_{xn} above and to describe a means of implementation.

Conditional frequency discriminator.- We now reconsider the estimator $\hat{M}_{pq}$ defined in equations (54) and (55). We restrict ourselves to the signal model given in equations (30) and (38) with* $\lambda_b = 0$ and with rarely overlapping bursts; i.e., $\alpha << 1/R$. This is the "low density" shot noise case discussed by Papoulis [10], page 574. For "low density" shot noise we may use the approximation that [10] if

$$s(t) = \Sigma h(t - \tau_j) \tag{87}$$

then

$$s^2(t) \approx \Sigma h^2(t - \tau_j) \tag{88}$$

with these constraints we obtain

$$\langle n_k n_{k-p}|\lambda(t)\rangle = \Delta\tau^2 \lambda(t)\lambda(t - p\Delta\tau) \tag{89}$$

$$= \Delta\tau^2 \sum_{j=-\infty}^{\infty} \lambda_j^2 f^2(t - \tau_j)\{1 + \cos \omega_j(t-\tau_j)$$

$$+ \cos \omega_j(t - \tau_j - p\Delta\tau) + \tfrac{1}{2} \cos(2\omega_j t - 2\omega_j\tau_j - p\omega_j\Delta\tau)$$

$$+ \tfrac{1}{2} \cos p\omega_j\Delta\tau\}$$

---

*The $\lambda_b = 0$ assumption does not affect the result due to the subtraction.

In equation (89) the product of cosine terms has been expanded as sum and difference frequency terms, and the delay $p\Delta\tau$ has been neglected in the envelope function f(t). With m_k defined by equation (55) we may determine $\langle m_k|\lambda(t)\rangle$ from two sets of terms like that in (89). We then determine $\langle\hat{M}_{pqn}\rangle$ as

$$\langle\hat{M}_{pqn}|\lambda(t)\rangle = \sum_{k=(n-1)L}^{nL} \langle m_k|\lambda(t)\rangle \tag{90}$$

$$\approx \frac{\Delta\tau}{2} \int_{(n-1)\Delta T}^{n\Delta T} \left\{ \sum_{j=-\infty}^{\infty} \lambda_j{}^2 f^2(t-\tau_j)[\cos p\omega_j\Delta\tau - \cos q\omega_j\Delta\tau] + [\text{Band pass terms}] \right\} dt$$

where

$$L = \Delta T/\Delta\tau \tag{91}$$

In the right hand side of this equation the sum is replaced by a time integral which it approximates. Since ΔT is long compared with the Doppler period, the bandpass terms average to a small value; however, since ΔT was assumed short compared with the burst envelope duration, the integral does not smooth the first expression in the right hand side of (90). The result is therefore

$$\langle\hat{M}_{pqn}\rangle \approx \frac{\Delta\tau\Delta T}{2} \sum_{j=-\infty}^{\infty} \lambda_j^2 f^2(t-\tau_j)[\cos p\Delta\tau\omega_j - \cos q\Delta\tau\omega_j] \tag{92}$$

$$= \frac{\Delta\tau\Delta T}{2} \lambda^2{}_{\ell p}(t)[\cos p\Delta\tau\omega(t) - \cos q\Delta\tau\omega(t)]$$

By proper selection of a high speed digital clock period, $\Delta\tau$, the sequence $\hat{M}_{pqn}$ approximates the sequence $\hat{M}_{sn}$ described

above for certain values of the integers p and q. For other choices of p and q the sequence $\hat{M}_{pqn}$ approximates the sequence M_{xn}. Thus, velocity correlations may be obtained by simultaneously duplicating the computations of (73) with two different sets of integers p and q, and then proceeding with software processing of the two sequences M_{sn} and M_{xn}. To show this last link in the procedure we examine the cosine difference term in (92). For the M_{sn} sequence we select p and q and adjust the variable $\Delta\tau$ to the conditions given previously for the mean frequency discriminator in equations (58) and (59).

$$(p - q)\omega_m\Delta\tau = \pi \tag{93}$$

$$p\omega_m\Delta\tau = 3\pi/2$$

$$q\omega_m\Delta\tau = \pi/2$$

Example selections for p, q and $\Delta\tau$ are $3,1,T_m/4$; $6,2,T_m/8$; $12,4,T_m/16$; where $T_m = 2\pi/\omega_m$ is inverse of the mean signal frequency. Expansion of the bracketed cosine term in (92) gives

$$[\cos p\Delta\tau\omega_j - \cos q\Delta\tau\omega_j] = \left[\sin\left(\frac{\pi\Delta\omega_j}{2\omega_m}\right) + \sin\left(\frac{3\pi\Delta\omega_j}{2\omega_m}\right)\right] \tag{94}$$

where we have used the substitutions

$$\Delta\omega_j = \omega_j - \omega_m \tag{95}$$

$$\cos\left[\frac{3\pi}{2\omega_m}(\omega_m + \Delta\omega_j)\right] = \sin\left(\frac{3\pi\Delta\omega_j}{2\omega_m}\right)$$

$$\cos\left[\frac{\pi}{2\omega_m}(\omega_m + \Delta\omega_j)\right] = -\sin\left(\frac{\pi\Delta\omega_j}{2\omega_m}\right)$$

Equation (94) was shown plotted in Figure 5 since it is also the approximate long-time average frequency transfer characteristic for the mean flow measurement. The trigonometric substitutions along with the small angle approximation $\sin\theta \simeq \theta$ show that for small turbulence levels, equation (92) becomes

$$\langle M_{sn} | \lambda(t) \rangle \simeq \Delta T \Delta\tau \lambda^2_{\ell p}(t) \pi \rho(t) \tag{96}$$

Where $\rho(t) \simeq \Delta\omega_j/\omega_m$ during non-zero portions of $\lambda_{\ell p}(t)$.

Normalizing sequence.- Under the same selection of $\Delta\tau$ as in (93) but with

$$p\omega_m \Delta\tau = 2\pi \tag{97}$$

$$q\omega_m \Delta\tau = \pi$$

a different effect is obtained. For example, if M_{sn} is obtained with $p = 3$, $q = 1$ and we let $p = 4$, $q = 2$ in computing M_{xn}, the result corresponding to (94) is

$$[\cos p\Delta\tau\omega_j - \cos q\Delta\tau\omega_j] = \left[\cos\left(\pi\frac{\Delta\omega_j}{\omega_m}\right) + \cos\left(2\pi\frac{\Delta\omega_j}{\omega_m}\right)\right] \tag{98}$$

The small-angle approximation for the cosine function is unity, so the result corresponding to (96) is

$$\langle M_{xn} | \lambda(t) \rangle = \Delta T \Delta\tau \lambda^2_{\ell p}(t) \tag{99}$$

When we note that $\Delta\omega_j/\omega_m = u_j/\bar{U}$ and that the $\Delta T\Delta\tau$ term cancels by division, we see from equations (96), (99) and (86) that the autocorrelation of M_{sn} divided by the autocorrelation of M_{xn} produces approximately $\pi^2\langle u(t)u(t+\tau)\rangle/\bar{U}^2$. Except for a factor of $C^2 = \pi^2$, the result is normalized in such a manner that

fractional mean-square turbulence intensity is directly obtainable from the first lag value of the final autocorrelation estimate or a projection back to the zero delay value. (The analysis we have presented is not valid for the zero delay value without separate consideration. It is possible that certain effects will cancel and cause this to be a valid point also.)

Practical considerations.- The approach outlined above for normalization would require as much hardware to measure the M_{xn} sequence as the M_{sn} sequence. In addition, the small angle approximation which was applied to (98) is not valid over a very large range of velocity deviation. We have conceived two other less expensive approaches. The first of these consists of eliminating the second M_{xn} channel completely and relying on the fact that the shape of the correlation $R_\rho(\tau)$ is approximated by correlating M_{sn} except in the vicinity of a burst duration from the delay origin. If it were desirable to normalize the function at the rest of the delay locations, we could evaluate the required division constant as

$$\Delta T^2 \Delta\tau^2 \pi^2 \langle \lambda^2_{\ell p}(t) \rangle^2 = \langle \hat{R}_s(n\Delta T) \rangle, \quad n\Delta T >> \alpha \qquad (100)$$

where we have already discussed a possible estimate for $\langle \lambda^2(t) \rangle$ in equation (46). Either this estimator or the M_{xn} approach described above could be computed with a single channel electronic system by electronically switching the delay variables p and q and storing the $\{\hat{R}_{pqn}\}$ sequences in different portions of a computer memory before computing the second level correlations. Time sharing like this would not be as efficient in possible cancellation of some of the statistical variability error, but significant cost savings would result.

DISCUSSION

System Design

We have provided a specification for an advanced computer controlled photon counting processor in Appendix D. The design allows the system to be operated as a dual-correlate and subtract processor or sequentially as a correlator by time sharing the multiplier. The system provides synchronous 3-bit X 3-bit operations at up to 100 MHz. The design uses "slow" emitter coupled logic (ECL) which is optimum for the speed range specified. The system may be operated as an advanced processor by dumping the accumulator values to computer memory at rates limited only by the computer. The design allows two identical units to be used together for either velocity cross-correlation measurements or for simultaneous second-channel normalization. An analog feedback loop is provided for automatic mean velocity acquisition. In addition, the system can be used to measure any type of multiple-interval photon statistics by selecting the correlator clock period (continuously variable both manually and electronically) and using the computer to sample the values of n_k stored in the delay line.

Sensitivity Comparison

There are four primary sources of variability error. These are the random turbulent flow itself, the random occurrence times of the scattering particles, the random scattering cross sections, and the random time of photon events. Photon correlation methods are linear in the sense that the effects of two simultaneously occurring scatterers are added. This is beneficial in that it avoids the non-linear zero-crossing capture effect of classical FM systems and thus the error problems

of multiple scatters; it is not beneficial in the sense that random amplitude effects will contribute to variability error, but these distinctions have not been carefully analyzed. The error versus data collection time trade-offs which result due to the random occurrence times of scatterers and due to minimum limits due to the turbulence itself have been previously analyzed for burst counters. That result* may be expressed as

$$T = \frac{\langle \rho^2 \rangle}{\langle \varepsilon^2 \rangle} \left(\frac{1}{R'} + \frac{1}{2B} \right) \tag{101}$$

where B is the equivalent power bandwidth of the turbulence, R' is the mean rate of accepted signal bursts, and $\langle \rho^2 \rangle$ and $\langle \varepsilon^2 \rangle$ are the normalized mean-square turbulence intensity and mean-square estimate error, respectively:

$$\langle \rho^2 \rangle = \frac{\langle u^2(t) \rangle}{\bar{U}^2} \tag{102}$$

$$\langle \varepsilon^2 \rangle = \frac{\langle (\hat{U} - \bar{U})^2 \rangle}{\bar{U}^2}$$

this result indicates, for example, that for a turbulence equivalent power bandwidth of 2KHz, 10% turbulence intensity, and 0.3% desired rms error, the data collection time would be at least 0.28 seconds even if the continuous signal U(t) were available for processing, and would be considerably longer if R' were less than 4000/sec.

In the following we examine the implications of equation (72) for transonic wind tunnel measurements. In order to include the mean value of the signal bursts along with the assumed

---

*page 10, equation (2.14), reference [23].

background light in equation (72) we use equation (40) for $\langle\lambda(t)\rangle$ and (72) becomes

$$\varepsilon \approx \frac{2(\lambda_b + \lambda_s)}{\alpha\sqrt{T\Delta\tau}\ R\langle\lambda_j^2\rangle\,\pi\sqrt{\pi}} \tag{103}$$

where the mean rate due to signal bursts is

$$\lambda_s = R\langle\lambda_j\rangle\sqrt{\pi}\,\alpha \tag{104}$$

which is less than the mean peak rate $\langle\lambda_j\rangle$ when R is less than the inverse of the effective burst width, $\sqrt{\pi}\,\alpha$. Now by defining the variance σ_λ^2 of the pedastal peak rates λ_j as

$$\sigma_\lambda^2 = \langle\lambda_j^2\rangle - \langle\lambda_j\rangle^2$$

we may rearrange (103) as

$$\varepsilon = \frac{2\left(\frac{\lambda_b}{\lambda_s} + 1\right)}{\langle\lambda_j\rangle\left[\frac{\sigma_\lambda^2}{\langle\lambda_j\rangle^2} + 1\right]\pi\sqrt{T\Delta\tau}} \tag{105}$$

Although the parametric behavior of equation (105) is intuitively acceptable in other ways, the presence of the term $[1 + \sigma_\lambda^2/\langle\lambda_j\rangle^2]$ in the denominator seems a little strange. Increased variability of the scattering cross sections of the particles would not intuitively decrease the mean-flow variability error. It is possible that this indicated behavior is a consequence of ignoring the variability of the classical power $\lambda(t)$ in equation (71) and has no physical reality. However, there does not appear to be anything wrong with the derivation

for the limiting case of high background light so the strange result may be true. In any event, a conservative bound is obtained by removing the bracketed expression in the denominator to obtain an expression not requiring knowledge of σ_λ^2:

$$\varepsilon \approx \frac{2\left[\frac{\lambda_b}{\lambda_s} + 1\right]}{\pi \langle\lambda_j\rangle \sqrt{T\Delta\tau}} \tag{106}$$

If we evaluate equation (106) with the following assumed typical conditions for a transonic wind tunnel measurement we obtain a required data collection time of 0.5 seconds for a 1% rms error:

$$\lambda_b = 10^7 \tag{107}$$

$$\lambda_s = 10^6$$

$$\langle\lambda_j\rangle = 10^7$$

$$\Delta\tau = 10^{-8}$$

In this example, the mean signal photoelectron rate is ten times less than the mean background photo-electron rate and is equal to the average peak envelope rate. With this much background light, the assumption of constant $\lambda(t)$ should be valid with respect to the photon-fluctuation induced variability. The selection of mean peak rate at 10^7 means that occurrences of photoelectron count rates greater than 10^8/sec (the limit of current hardware state of the art) will be rare and the effects of nonlinearity negligible). The selected ratio of $\langle\lambda_j\rangle/\lambda_s = 10$ implies that the measurement volume is only assumed to contain a scatterer 1/10 of the time on the average.

Even though dramatic improvements over the previous example situation may result from reduced background light, the result still indicates that practical measurements may be obtained with a peak signal photoelectron rate of 10^7 sec. In order to compare this with the performance of a burst-counter system, we must assume values for p, q and f_m, the Doppler frequency. With p = 3, and q = 1 the Doppler frequency f_m is $1/4\Delta\tau$ = 25 MHz. This would result from $\bar{U}$ = 304.8 m/sec with an optical sensitivity of 82 kHz/m/sec. This peak photoelectron rate assumed is thus 0.4 photoelectrons/cycle in the presence of 0.4 background photoelectrons/cycle. For comparison we note that standard optical noise formulas, given $\lambda(t) = \lambda_j(1 + \cos \omega_m t) + \lambda_b$, would result in peak SNR of

$$\text{SNR} = \frac{\lambda_j^2}{4B(\lambda_j + \lambda_b)} \qquad (108)$$

In our example, B = 25 MHz and $\lambda_b = 10^7$; if we choose $\lambda_j = 10^9$, a factor of 100 greater than in our example, then the SNR is 10 at the peak of the signal burst and 1.35 at the 1/e signal envelope points. Since this example represents marginal or inadequate SNR for burst counter operation we deduce that, even with 100 times more scattered power, only the larger-than-average scatterers would contribute.

Under conditions of less background light, the burst-counter analysis would not be improved; however, the photon counting system results are expected to improve considerably. Thus we conclude that mean-flow measurements with from 100-1000 times less optical power are feasible with the photon counting system.

During this contract effort we have developed simulation techniques which can be extended to be applicable to all types of LV signal processors for any level signals. The program in Appendix B only represents the beginning of how these techniques can be exploited, and we did not have time under the present contract to use that program except for check-out waveform simulations and the dead-time example. Similarly, the higher order moment equations developed in Appendix A have not been yet used to extend the variability error analysis to include the low background case.

A system such as that specified in Appendix D should be constructed and tested. The results in this report indicate that such a system would a low LV measurements to be performed which are not now feasible. In addition, the system would be a valuable research tool for many other fields of research which require high-speed digital correlation or measurement of photon interval statistics.

CONCLUSIONS

The most significant new results which this report provides are itemized below:

- A general non-stationary Poisson process model for dual scatter laser velocimeter (LV) signals and noise valid from high level signals down through photon resolved signals.
- Computer simulation algorithms valid over the entire range of signal levels, which may be used to evaluate any new type of LV signal processor.
- A description and statistical analysis of both conventional photon correlation and Dual Correlate and Subtract frequency discriminator technique for mean, turbulence intensity and turbulence correlation estimations from photon resolved signals.
- A system design for an advanced photon-counting processor which implements both conventional photon correlation (sequentially) and the Dual Correlate concepts with time resolution to 10 nsec.

APPENDIX A

FILTERED INHOMOGENEOUS POISSON PROCESSES

In this appendix we have used the material from Snyder's book [9] to derive the higher order moments of a filtered inhomogeneous Poisson process up through order 4. We begin with introductory material similar to that given by Papoulis [10].

Inhomogeneous Impulse Processes

The input to a random linear system is an inhomogeneous Poisson impulse process z(t) given by

$$z(t) = \sum_{-\infty}^{\infty} \delta(t - \tau_i) \tag{A1}$$

where $\{\tau_i\}$ is the set of random occurrence times, $\lambda(t)$ is the instantaneous statistical mean value of z(t), (and also the mean rate of occurrence of the τ_i's), and $\delta(t)$ is the dirac delta function. The random variables τ_i are independent of each other statistically and obey the inhomogeneous counting law, i.e., the probability of n = k occurrences in the interval (t_1, t_2) is

$$P\{n(t_1, t_2) = k\} = \frac{e^{-\mu} (\mu)^k}{k!} \tag{A2}$$

where

$$\mu = \int_{t_1}^{t_2} \lambda(t) dt \tag{A3}$$

The quantity μ is also the mean and variance of the random variable $n(t_1, t_2)$.

The Response of a Random Linear System-Campbell's Theorem

The output of the random linear system s(t) is the superposition of the response $h(t - \tau_i, \bar{Y}_i)$ to each input impulse:

$$s(t) = \sum_{-\infty}^{\infty} h(t - \tau_i, \bar{Y}_i) \qquad (A4)$$

where $\{Y_i\}$ is a set of identically distributed independent vector random variables. The random variable $\bar{Y}$ affects the shape and amplitude of the response function $h(t,\bar{Y})$. In the case of the PMT signal it may take the form of a single scalar amplitude variable. In the case of the classical optical signal from turbulent flow both a random amplitude parameter and one or more random shape parameters due to velocity magnitude, direction, and probe volume translational entrance location may be required. The theory should be applicable so long as the set of multidimensional random variables $\bar{Y}_i$ is independent of the set of occurrence times $\{t_i\}$. The generalized Campbell's theorem results for the instantaneous statistical mean, variance, and auto-covariance of s(t) are given below, they apply regardless of whether individual pulses are resolved or not.

$$\langle s(t)\rangle = \int_{-\infty}^{\infty} \lambda(\tau)\langle h(t - \tau,\bar{Y})\rangle d\tau \qquad (A5)$$

$$\sigma_s^2(t) = \langle s^2(t)\rangle - \langle s(t)\rangle^2 = \int_{\infty}^{\infty} \lambda(\tau)\langle h^2(t - \tau,\bar{Y})\rangle d\tau \qquad (A6)$$

$$\begin{aligned} \mathrm{cov}[s(t_1)s(t_2)] &= \langle s(t_1)s(t_2)\rangle - \langle s(t_1)\rangle\langle s(t_2)\rangle \qquad (A7) \\ &= \int_{\infty}^{\infty} \lambda(\tau)\langle h(t_1 - \tau,\bar{Y})h(t_2 - \tau,\bar{Y})\rangle d\tau \end{aligned}$$

where $\langle\rangle$ denotes expectation with respect to $\bar{Y}$ inside the integral signs. For a causal signal such as that from the PMT, where h(t) is zero for $t > 0$, then the upper limits of

integration may be replaced by t or the minimum of t_1 and t_2 in equation (A7). For the transient case where the impulse signal z(t) is applied at t = 0, the lower limits of integration may be replaced by 0.

Higher Order Moments

Summary of statistics.- Given a filtered, inhomogeneous, compound Poisson process:

$$s(t) = \sum_{-\infty}^{\infty} h(t,\tau_i;\overline{Y}_i) \tag{A8}$$

where τ_i are random occurrence times which occur with intensity $\lambda(t)$, and where $\overline{Y}_i$ are vector random variables which are statistically independent and identically distributed, we obtain the following result. The cumulants are:

$$\gamma_1(t_1) = \eta_1 = \int_{\infty}^{\infty} \lambda(\tau) \langle h(t_1,\tau;\overline{Y}) \rangle \, d\tau \tag{A9}$$

$$\gamma_{12}(t_1,t_2) = \mu_{12} = \int_{\infty}^{\infty} \lambda(\tau) \langle h(t_1,\tau;\overline{Y}) h(t_2,\tau;\overline{Y}) \rangle d\tau$$

$$\gamma_{123}(t_1,t_2,t_3) = \int_{\infty}^{\infty} \lambda(\tau) \langle h(t_1,\tau;\overline{Y}) h(t_2,\tau;\overline{Y}) h(t_3,\tau;\overline{Y}) \rangle d\tau$$

$$\gamma_{1234}(t_1,t_2,t_3,t_4) = \int_{\infty}^{\infty} \lambda(\tau) \langle h(t_1,\tau;\overline{Y}) h(t_2,\tau;\overline{Y}) \cdot h(t_3,\tau;\overline{Y}) h(t_4,\tau;\overline{Y}) \rangle \, d\tau$$

The formulas which relate the cumulants to the moments are as follows:

1. $\langle s(t_1) \rangle = \eta_1 = \gamma_1$ (A10)

2. $\langle s(t_1) s(t_2) \rangle = \mu_{12} + \eta_1 \eta_2$
   where μ_{12} = covariance = γ_{12}

3. $\langle s(t_1)s(t_2)s(t_3)\rangle = \gamma_{123} + \eta_1\mu_{23} + \eta_2\mu_{13} + \eta_3\mu_{12} + \eta_1\eta_2\eta_3$

4. $\langle s(t_1)s(t_2)s(t_3)s(t_4)\rangle = \gamma_{1234} + \eta_1\eta_2\eta_3\eta_4 + \eta_1\gamma_{234} + \eta_2\gamma_{134} + \eta_3\gamma_{124} + \eta_4\gamma_{123} + \mu_{12}\mu_{34} + \mu_{13}\mu_{24} + \mu_{14}\mu_{23} + \mu_{14}\eta_2\eta_3 + \mu_{13}\eta_2\eta_4 + \mu_{12}\eta_3\eta_4 + \mu_{24}\eta_1\eta_3 + \mu_{23}\eta_1\eta_4 + \mu_{34}\eta_1\eta_2$

The derivation of the above formulas follows.

Derivation.- The derivation of the preceding formulas is straightforward but tedious if we are given the joint characteristic function

$$\phi(\bar{\omega}) = \langle e^{j\bar{\omega}\cdot\bar{s}} \rangle \tag{A11}$$

where

$$\bar{\omega} = (\omega_1, \omega_2, \omega_3, \omega_4) \tag{A12}$$

and

$$\bar{s} = [s(t_1), s(t_2), s(t_3), s(t_4)] \tag{A13}$$

From Papoulis we know that

$$\langle s(t_1)s(t_2s(t_3)s(t_4)\rangle \tag{A14}$$

$$= \frac{1}{(j)^4} \frac{\partial^4 \phi(\bar{\omega})}{\partial\omega_1 \partial\omega_2 \partial\omega_3 \partial\omega_4}\Bigg|_{\bar{\omega}=0}$$

and similarly for other moments; i.e., we may obtain the moments by determining the appropriate partial derivatives of the joint characteristic function at $\bar{\omega} = 0$ which is in turn a vector valued Fourier transform of the joint probability function for the random variables $s(t_1)$, $s(t_2)$, etc.

The theory of filtered Poisson processes provides us with the joint characteristic function of the second kind, ψ, where

$$\psi(\bar{\omega}) = \ell n\ \phi\ (\bar{\omega}) \tag{A15}$$

or

$$\phi(\bar{\omega}) = e^{\psi(\bar{\omega})} \tag{A16}$$

We may therefore either write out $\phi(\bar{\omega})$ and evaluate the derivatives directly or use the above equations to first express the partial derivatives of $\phi(\bar{\omega})$ in terms of the partial derivatives of $\psi(\omega)$. We have taken the latter approach using the chain rule. As an example

$$\frac{\partial^2 \phi}{\partial\omega_1 \partial\omega_2} = \phi \cdot \left(\frac{\partial^2 \psi}{\partial\omega_1 \partial\omega_2} + \frac{\partial\psi}{\partial\omega_1} \frac{\partial\psi}{\partial\omega_2}\right) \tag{A17}$$

The rest of the derivatives are omitted here since they get progressively more lengthy.

We now need only to evaluate the products of partial derivatives we have obtained at $\bar{\omega} = 0$. From the material given

by Snyder* we have

$$\psi(\bar{\omega}) = \int_{-\infty}^{\infty} \lambda(\tau) \langle e^{j\beta(\bar{\omega})} - 1 \rangle \, d\tau \qquad \text{(A18)}$$

where

$$\beta(\bar{\omega}) = \omega_1 h(t_1, \tau; \bar{Y}) + \omega_2 h(t_2, \tau; \bar{Y}) + \ldots + \omega_n h(t_n, \tau; \bar{Y}) \qquad \text{(A19)}$$

From the form of the expression for $\psi(\bar{\omega})$ it is clear that

$$\bar{\psi}(\bar{\omega})\Big|_{\bar{\omega}=0} = \int_{-\infty}^{\infty} \lambda(\tau) \langle e^{j0} - 1 \rangle \, d\tau = 0 \qquad \text{(A20)}$$

therefore

$$\phi(\bar{\omega})\Big|_{\bar{\omega}=0} = 1 \qquad \text{(A21)}$$

It is not difficult to see that the form of the partial derivatives is

$$\frac{\partial^n \psi(\bar{\omega})}{\partial\omega_1 \partial\omega_2 \ldots}\Big|_{\bar{\omega}=0} = j^n \int_{-\infty}^{\infty} \lambda(\tau) \, \langle h(t_i, \tau; \bar{Y}) h(t_2, \tau; \bar{Y}) \ldots e^{j\beta(\bar{\omega})} \rangle dt \Big|_{\bar{\omega}=0} \qquad \text{(A22)}$$

i.e., the partials of $\psi(\bar{\omega})$ at $\bar{\omega} = 0$ are equal to the same order cumulant except for the j^n factor. With this formula we can now go directly from the expression of the partials of ϕ in terms of the partials of ψ to the desired higher order moments. The result is that given in the summary. If moments higher

---

*In Snyder's book, Random Point Processes, equation (4.15) the lower limit of integration is to correspond to the beginning of the process. The upper limit is the minimum of the times t_i. This assumes that $h(t_i, \tau; \bar{Y})$ is a causal function.

than the 4th are needed we would simply apply the chain rule to determine the higher derivative of ϕ in terms of those of ψ.

Moments of a Gaussian Random Process.- We have not yet expanded all of the moments of a non-zero mean Gaussian process for comparison. We observe, however, that the factorization property of zero-mean Gaussian processes does not hold for filtered Poisson process. Otherwise there are great similarities except for the cumulants as

Gaussian	Poisson	(A23)
$\langle x_1 \rangle = \eta_1$	$\langle x_1 \rangle = \eta_1$	
$\langle x_1 x_2 \rangle = \mu_{12} + \eta_1 \eta_2$	$\langle x_1 x_2 \rangle = \mu_{12} + \eta_1 \eta_2$	
for $(\eta_1 = 0)$		
$\langle x_1 x_2 x_3 \rangle = 0$	$\langle x_1 x_2 x_3 \rangle = \gamma_{123}$	
$\langle x_1 x_2 x_3 x_4 \rangle = \mu_{12}\mu_{34} + \mu_{13}\mu_{24} + \mu_{14}\mu_{23}$	$\langle x_1 x_2 x_3 x_4 \rangle = \mu_{12}\mu_{34} + \mu_{13}\mu_{24} + \mu_{14}\mu_{23} + \gamma_{1234}$	
$(\eta \neq 0)$		
$\langle x^4 \rangle = 3\sigma^4 + 6\sigma^2\eta^2 + \eta^4$	$\langle x^4 \rangle = 3\sigma^4 + 6\eta^2\sigma^2 + \eta^4 + 4\eta \int \lambda h^3(t)dt + \int \lambda h^4(t)dt$	

APPENDIX B

DIGITAL SIMULATION OF LOW LEVEL DUAL SCATTER LV SIGNALS AND IDEALIZED PHOTON PROCESSORS

This appendix provides theory and an example FORTRAN program for digital LV signal simulation. Background theory and several more complicated Poisson impulse simulation algorithms are discussed by R. H. Forrester, Jr. in a Masters Thesis [25] performed under Don Snyder. The simple approach taken here is to discretize the possible occurrence times of photon and classical burst signal events to uniformly spaced intervals of length Δt, where Δt is less than any significant system integration time. This discretization of time imposes itself upon all temporal system parameters, such as processor clock interval $\Delta\tau$ and dead time τ_d, which would be continuous variables in the real situation.

Theory

Realization of inhomogeneous Poisson impulse processes.- A sample function of an inhomogeneous Poisson impulse process is specified by a set of event occurrence times $\{t_i\}$ as described in Appendix A. The key procedure required for simulation of LV signals is therefore the generation of a set $\{t_i\}$ given a specified rate intensity function $\lambda(t)$. This may be done by first generating a homogeneous (stationary) process with unit intensity $\lambda(t) = 1$ and then mapping the realization times through solution of an integral equation. Figure B1 illustrates the required mapping in a manner which helps provide intuitive grasp for what follows.

Let us define the set of interarrival intervals $\{w_i\}$ between event occurrence times $\{\tau_i\}$ as

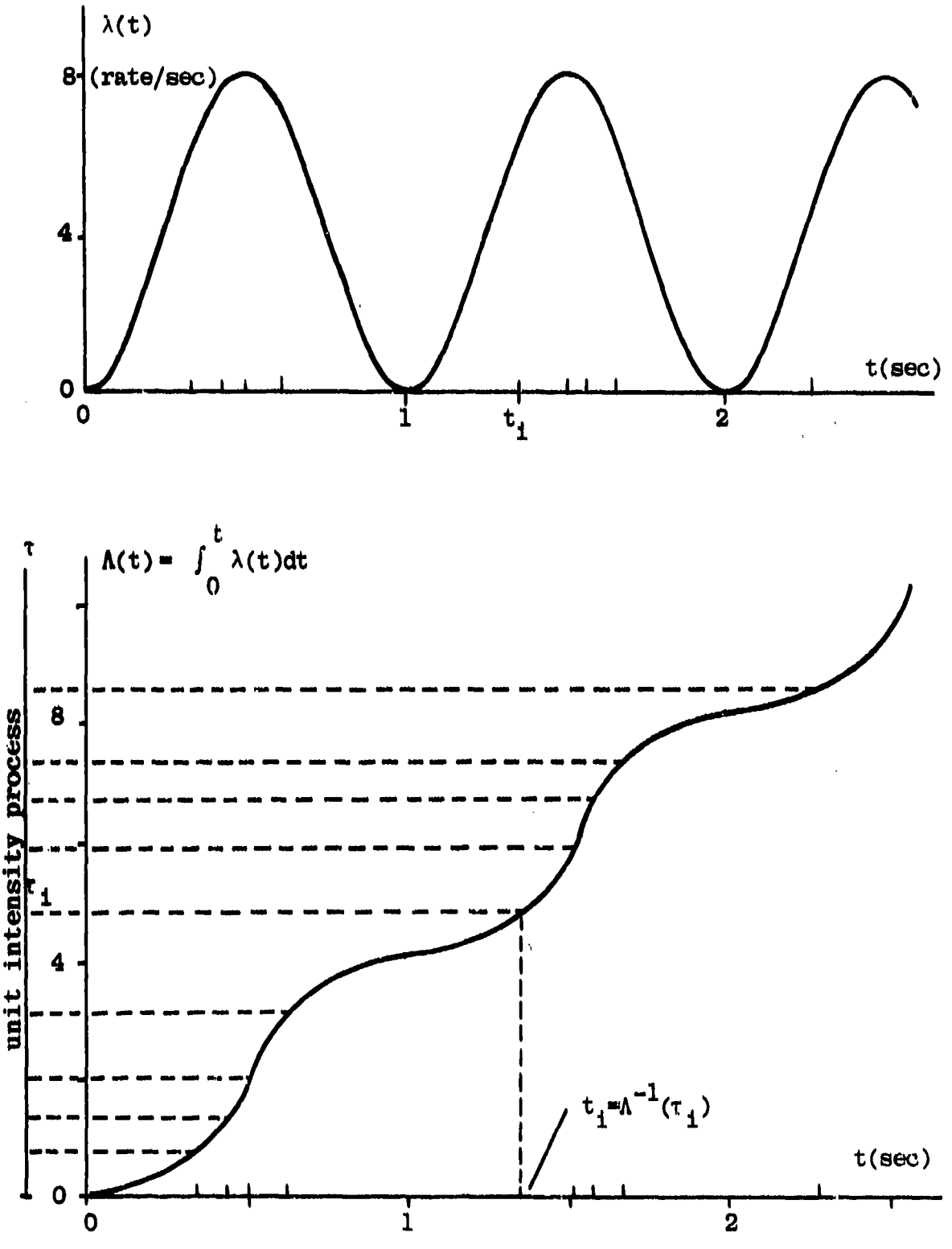

Inhomogeneous Process with λ(t)

Figure B1. Transformation of Unit Intensity Process into Inhomogeneous Process with Specified λ(t).

$$w_i = \tau_i - \tau_{i-1} \tag{B1}$$

For a homogeneous Poisson impulse process with constant rate intensity $\lambda(t) = \lambda$, it is necessary and sufficient that $\{w_i\}$ be a set of statistically independent, identically distributed exponential random variables with common probability density $p_w(w)$, given by

$$p_w(w) = \lambda e^{-\lambda w} \tag{B2}$$

We may therefore generate the set $\{\tau_i\}$ of occurrence times for a realization of a constant intensity process as

$$\tau_i = \sum_{k=1}^{i} w_k = \tau_{i-1} + w_i \tag{B3}$$

Commonly available subroutines* generate statistically independent realizations x_i of a random variable x uniformly distributed on the interval (0,1). The exponential density function is monotonic with an inverse function which is commonly available (namely the natural logarithm function). It is therefore straightforward to determine a transformation which maps the realizations of the unit uniformly distributed variable to the desired exponentially distributed variable:

$$w_i = \frac{1}{\lambda} \ln\left(\frac{1}{x_i}\right) \tag{B4}$$

In summary, generation of unit uniform random variables x; which are then transformed by (B4) and used in (B3) produce a

*There is, however, a difference in the quality of these subroutines; a survey paper by [26] may be consulted if the validity or efficiency of a subroutine is in question.

realization of a homogeneous impulse process with intensity λ. For our purposes, we set $\lambda = 1$ and proceed to the mapping step illustrated in Figure B1.

In his recent book* Snyder provides guidance, but leaves it as a homework exercise to deduce the proof for a method of rescaling the interarrival times of a unit intensity process to obtain a realization of a specified inhomogeneous process. The results are as follows: Let $\{\tau_i\}$ be the set of occurrence times of a unit intensity process as illustrated in Figure B1. Let $\Lambda(t)$ be the integral of the specified intensity function $\lambda(t)$:

$$\Lambda(t) = \int_0^t \lambda(\alpha)d\alpha \qquad \text{(B5)}$$

This function is continuous and monotonically increasing and therefore has an inverse function Λ^{-1} such that

$$\tau_i = \Lambda(t_i) \qquad \text{(B6)}$$

$$t_i = \Lambda^{-1}(\tau_i) \qquad \text{(B7)}$$

The set of times $\{t_i\}$ generated by applying equation (B7) to the set $\{\tau_i\}$ is the required realization of the inhomogeneous process.

Algorithm for simulation of event times.- The subroutines which generate uniform random variables x_k produce real numbers. If the above equations are applied exactly, one would be forced to digitally solve an integral equation, thus producing another set of real numbers $\{t_i\}$. One could carry the full resolution

---

*See Snyder [9] page 62.

of the computer to the bitter end of the simulation. However, at some point the use of digital filtering techniques to simulate analog filter characteristics of real photomultiplier tubes (PMT) and other electronic devices would become appropriate. At such a point, the simulated signal would have to be interpolated and respecified on uniformly spaced increments with separation Δt. We may greatly simplify the required algorithms by rounding the set of occurrence times to the nearest Δt interval and point. By incorporating this step directly into the solution of the inverse function $\Lambda^{-1}(\tau_i)$ we avoid the problems of solving the integral equation exactly and simplify that step as well. The entire procedure is thus simplified to the following.

1. Select a Δt small enough to provide adequate accuracy for uniform sampling of $\lambda(t)$ and calculating its integral by the trapazoidal rule integration method.

2. Beginning at $\tau_o = t_o = 0$, compute realizations of τ_i as discussed above.

3. Calculate the trapazoidal rule approximation of $\Lambda(k\Delta t)$ for each integer value. $0 \leq k \leq k_{max}$.

4. Use conditional statements to test the latest real value of τ_i against the integral $\Lambda(k\Delta t)$ as it is generated iteratively to determine a histogram TC of the discretized occurrence times at $k\Delta t$. It is possible, in the simulation, for more than one value of τ_i to be mapped to the discretized time $k\Delta t$.

There are many ways that the fourth step could be implemented. We have elected the following: If the value of τ_i lies in the range

$$\frac{\Lambda(k\Delta t) + \Lambda[(k-1)\Delta t]}{2} \leq \tau_i \leq \frac{\Lambda[(k+1)\Delta t] + \Lambda(k\Delta t)}{2} \qquad (B8)$$

where $\Lambda(k\Delta t)$ is the trapazoidal approximation of the integral,

then an occurrence is added to the histogram value at k.

Inclusion of random amplitude effects.- When the point event represents a photoelectron pulse or a classical LV signal burst, we may wish to assign the event an amplitude mark (impulse weight). This may be done by separately generating realizations of additional random variables according to desired statistics and accumulating one each of these at TC for each occurrence time. Note that it is not adequate to simply multiply each value TC by a random variable, since in some realizations more than one event contributes to the same value of k.

The statistics of the pulse height distribution of a poor (PMT) may be nearly Rayleigh, while the Gaussian density with 15-25% relative standard deviation may be adequate to model a good PMT. Very little documentation exists concerning the probability density of the classical signal bursts. This topic is discussed and some data is presented in our recent AEDC report [1]. Of the simplest densities an exponential density or a Rayleigh density would be used to simulate amplitudes from an unseeded flow. As we have shown it does not follow that the amplitude probability density agrees in any recognizable way with the particle size distribution; even monosized particles may produce a very strange amplitude probability density [1].

When it is desirable to use Rayleigh or Gaussian random variables the following procedure is recommended. Generation of realizations of Rayleigh or Gaussian random variables may be obtained by first generating uniformly distributed values on the interval (0,1). Let x_1 and x_2 be two such independent realizations. Then we obtain

$$R = (-2\sigma^2 \ln x_1)^{1/2} \tag{B9}$$

$$\theta = 2\pi x_2 \tag{B10}$$

where R is a realization of a Rayleigh random variable with parameter σ, mean = $\sigma\sqrt{\frac{\pi}{2}}$, and probability density $p_R(R)$ given as

$$p_R(R) = \frac{R}{\sigma^2} e^{-(R^2/2\sigma^2)}, \quad R \geq 0 \tag{B11}$$

and θ is a realization of a uniformly distributed random variable on the interval $(0, 2\pi)$. Multiplying (B9) by $\sqrt{2/\pi}$ produces Rayleigh variables with mean =1. If Gaussian random variables are desired, the process is continued from (B9) without the $\sqrt{2/\pi}$ factor by converting to rectangular co-ordinates:

$$X = R \cos \theta \tag{B12}$$

$$Y = R \sin \theta \tag{B13}$$

When this is done, X and Y are two independent realizations of a Gaussian random variable with zero mean and variance σ^2, i.e.,

$$p_x(X) = \frac{1}{\sqrt{2\pi}} e^{-x^2/2\sigma^2} \tag{B14}$$

and the same form for $p_y(Y)$. The above procedure efficiently produces exactly Gaussian random realizations as opposed to a program such as GAUSS which sums 12 independent uniform random variables to obtain approximately Gaussian variables by the central limit theorem (Forrester [25]).

Example Simulation Program

We have included at the end of this appendix a copy of the printout of a FORTRAN IV program which is illustrated in flow form in Figure B2. The occurrence times of the classical signal bursts are generated as a homogeneous Poisson process. The amplitudes of the bursts may be either generated randomly

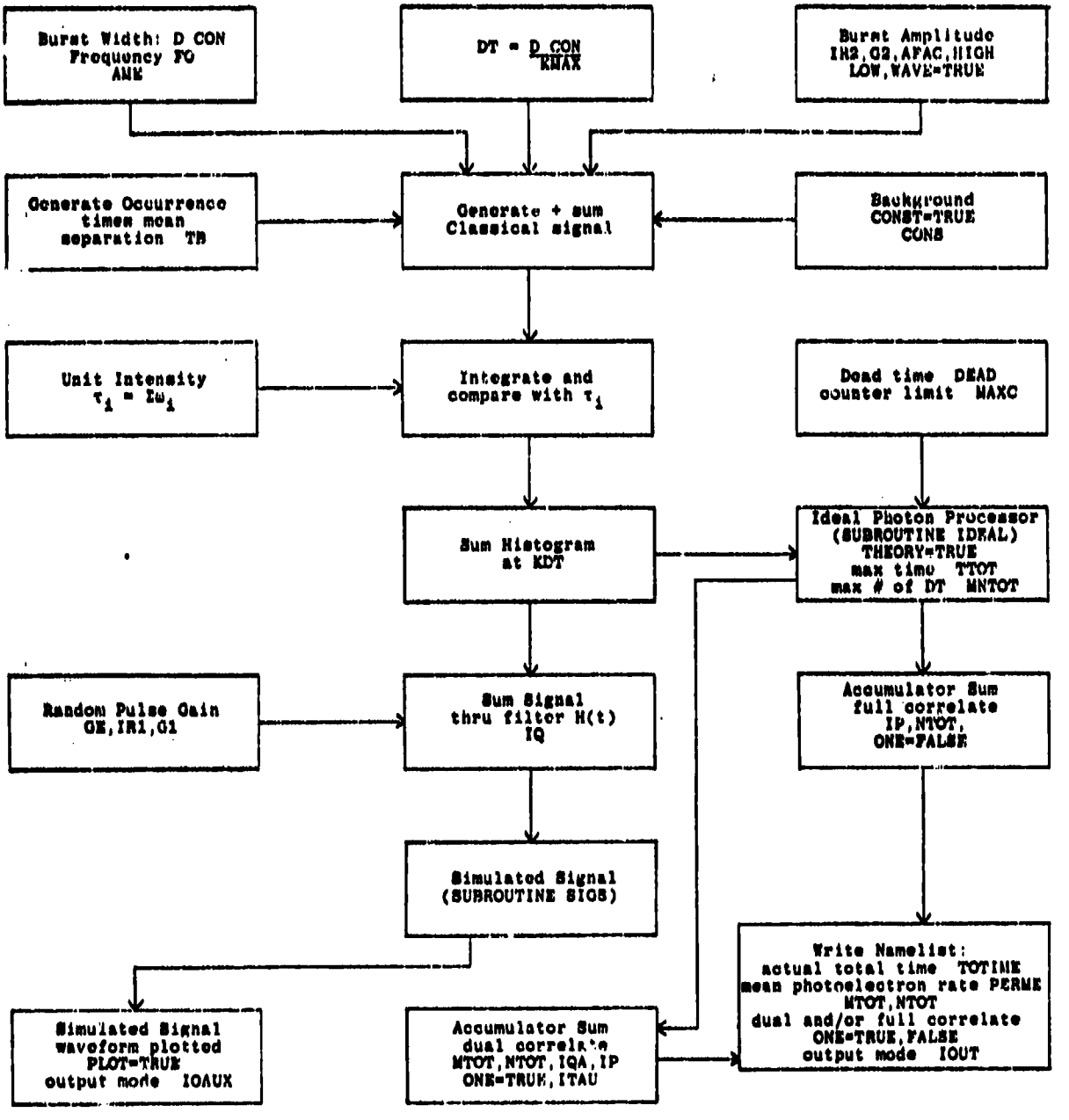

Figure B2. Flowchart Showing Namelist Variable Names and Functions.

with exponential, Gaussian, or Rayleigh density with a specified mean, or they may be set equal to a constant. The program computes the burst waveforms at each Δt and sums all that are present to form a classical signal. This signal is integrated in a trapazoidal fashion and compared with the occurrence times of a unit intensity homogeneous Poisson impulse process simulated as described previously. If random amplitudes have been assigned to the photoelectron pulses, these are generated and added to a histogram; otherwise 1's are added to the histogram.

The idealized photon processor portion of the program sums the values of the histogram (with no random PMT pulse height effects) over an interval $\Delta\tau$ which is some selected integral number (ITAU) of Δt units in length. The sum is the photon count sequence referred to in the text as $\{n_k\}$. The ideal processor then computes either the photon correlation for delay values 0-IP (ONE = false) or computes and sums the dual correlate and subtract terms (ONE = true).

```
1020*      LOGICAL PLOTS,THEORY,ZEROS,INSECT,WAVE,CONST,TEST,ONE,DONE
1030*      INTEGER OTIME,DTIME,DEAD
1035*      REAL HIGH,LOW
1040*      COMMON /SINE/ MKX(20),ONE,DONE,IOTV,IOTTOT,MNTOT
1050*      COMMON /IDEA/ TCR(1000),ZEROS,N(2000),ITCR(10),INSECT
1060*      COMMON /THEOR/ RC(1000),GE
1065*      COMMON /ADD/ MAXC,G1,G2
1070*      COMMON S(1000),IC(1000),X(47),JV,PHI,PLO
1080*      DATA TTOT,KMAX,IW,D,CON,AME,FO,CONS/50.E-6,480,2,8.E-7,3.0,
1085*     1 1.0,6.25E6,4.E9/
1090*      DATA AFAC,HIGH,LOW/4.E9,10.0,0.1/
1100*      DATA IR1,IR2/1,4/
1110*      DATA IN,IOUT,IOAUX/7,7,7/
1120*      DATA ITAU,IR,IQA,IP,NTOT,MTOT,DEAD/4,0,2,20,0,0,0/
1125*      DATA TB,PLOTS,THEORY,WAVE,CONST/5.E-6,
1128*     .FALSE.,.TRUE.,.TRUE.,.TRUE./
1130*      GE=5.E-3
1140*      JV=1
1150*      MAXC=1000
1155*      ZEROS=.FALSE.
1160*      ONE=.FALSE.
1165*      DONE=.FALSE.
1170*      INSECT=.FALSE.
1180*      G1=0.25
1190*      G2=0.25
1200*      MNTOT=1000
1210*      PLO=0.0
1220*      PHI=0.20
1230*C     LIST OF NAMELIST VARIABLE NAMES AND THERE MEANINGS...
1240*C     DT          = SMALLEST TIME INTERVAL USED IN SIMULATION
1250*C                   ALL TIME MEASURED IN INTEGER MULTIPLES (D*CON/KMAX)
1260*C     IOTIME      = TOTAL TIME OF SIMULATION IN SECONDS(ACTUAL)
1270*C     PERMT       = MEAN PHOTOELECTRON RATE
1275*C     MNTOT       =TOTAL # OF PHOTONS IN THE SIMULATION
1280*C     TTOT        = TOTAL TIME OF SIMULATION IN SECONDS(INPUT VARIABLE)
1290*C     KMAX        = TOTAL NUMBER OF DT S PER BURST
1300*C      IW         = THE WIDTH OF THE IMPULSE RESPONSE H(T) IS 2IW DT
1310*C                   ( H(T) IS TRIANGULAR FROM -IW DT TO +IW DT )
1320*C      AFAC       = MEAN PEAK RATE OF A SIGNAL BURST (MEAN PEAK LAMBDA)
1330*C      HIGH       = HIGH BOUND FOR PEAK LAMBDA (HIGH*AFAC)
1340*C      LOW        = LOW BOUND FOR PEAK LAMBDA (LOW*AFAC)
1350*C      IR1        =SELECTS TYPE OF RANDOM VARIABLE FOR PHOTOELECT. PULSES
1355*C      G1         =GIVES THE SIGMA VALUE OF THE GAUSIAN RANDOM VARIABLE
1360*C      IR2        =SELECTS TYPE OF R.V. FOR THE CLASSICAL BURST HEIGHTS
1365*C      G2         =GIVES THE SIGMA VALUE OF THE GAUSIAN FOR IR2
1370*C      TB         = MEAN SIGNAL BURST SEPERATION ROUNDED TO
1380*C                   INTEGER NUMBER OF DT S (IN SECONDS)
1390*C     PLOTS       = LOGICAL OPERATOR WHICH PLOTS OUTPUT WHEN SET TRUE
1392*C     PHI         = HIGH BOUND FOR THE PLOTS ROUTINE
1394*C     PLO         = LOW  BOUND FOR THE PLOTS ROUTINE
1400*C     THEORY      = LOGICAL WHICH USES IDEAL PROCESSOR WHEN SET TRUE
1405*C     MAXC        = LIMIT OF THE COUNTER IN THE IDEAL PROCESSOR
1410*C     IOUT        = SPECIFIES THE OUTPUT FILE
1420*C     IOAUX       = SPECIFIES AN AUXILARY OUTPUT FILE FOR PLOTS
1430*C     D           = THE 1/E SQUARED HALF WIDTH (SECONDS) OF BURST
1440*C     CON         = DETERMINES WHERE BURST IS TRUNCATED TO ZERO
1450*C                   (TOTAL WIDTH= CON*D)
1460*C     AME         = MODULATION INDEX FOR BURSTS(E**(-2T**2/D**2)*
1460*C                   (1+ AME COS(2PIE FO T))
1460*C     FO          = BURST SIGNAL FREQUENCY
1490*C     ITAU        = THE INTEGER NUMBER OF DT S COMPRISING ONE PROCESSOR
1500*C                   DTAU
1510*C     IR          = THE REMAINDER OF AN INTEGER DIVISION OF THE NUMBER
1520*C                   OF DT S BY ITAU
1530*C     IQA         = SECOND CORRELATION DELAY INDEX AS USED IN
1540*C                   NS(2(NS-IP)-NS-IQA))
1550*C     IP          = CORRELATION DELAY INDEX MAXIMUM OR FIRST VALUE IN
1560*C                   DUAL CORRELATE
1570*C     NTOT        = SUM OF PHOTOELECTRONS COUNTED DURING TOTAL MEASUREMENT
1580*C     MTOT        = ACCUMULATOR SUM
1590*C     WAVE        = LOGICAL WHICH IS SET TRUE WHEN A CLASSICAL BURST IS
1600*C                   PRESENT
1610*C     CONST       = LOGICAL WHICH IS SET TRUE WHEN A CONSTANT BACKGROUND
1620*C                   IS PRESENT
```

```
C= CONS     = THE CONSTANT BACKGROUND LAMBDA TO BE ADDED IN THE TRUE
C=            CONDITION OF CONST
C= DEAD     = THE INTEGER NUMBER OF DT S OF THE DEAD TIME INTERVAL
C=              IF NOT USED THEN IT DEFAULTS TO ZERO.
C= ONE      = LOGICAL WHERE TRUE DUAL CORRELATE,FALSE IMPLIES
C=                         IP IS THE MAX DELAY IN PHOTON CORRELATION.
C= GE       = PRODUCT OF ELECTRONIC CHARGE AND CHARGE GAIN G FOR PMT
   NAMELIST /INP/ICLT,IDAUX,THEORY,PLOTS,PHI,PLO,WAVE,CONST,CONS,ONE,
-  D,CON,KMAX,TB,AFAC,HIGH,LOW,IR1,G1,IR2,G2,IQ,GE,AME,FO,IQA,
-  IP,MAXC,DEAD,ITAU,TTOT,MNTOT,TOTIME,NTOT,PERME,MTOT,DT
C=
C=  READ IN PROGRAM VALUES WITH A NAMELIST READ
C=
    READ(IN,INP)
    FAC=TB/D/CON*KMAX
    DT=D*CON/KMAX
    IDTTOT=TTOT/DT
    DTIME=RAND(1,JV,G2)*FAC
    OTIME=0
    IPOINT=1
    M=4
C= PERFORM A SIMULATION FOR NSB SIGNAL BURSTS(# OF BURST LOOPS)
    999 CONTINUE
C= GET A RANDOM VALUE FOR THE PEDASTAL PEAK LAMBDA GENERATION
    15 AMP=RAND(IR2,JV,G1)*AFAC
C= IF THIS VALUE IS NOT IN PEAK LAMBDA BOUNDS (HIGH,LOW)*AFAC
C= THEN GO BACK AND TRY AGAIN
    IF(AMP.GT.(AFAC*HIGH).OR.AMP.LT.(AFAC*LOW))GO TO 15
    JEND=DTIME-OTIME
C= DETERMINE IF THERE IS SPACE IN BETWEEN THE SIGNAL BURSTS
C= ****THIS BRANCH IS USED FOR SPACING OR FILLER IN BETWEEN
C=                     SIGNAL BURSTS****
    IF(JEND.LE.0)GO TO 35
    IF(.NOT.PLOTS.OR.CONST)GO TO 99
    DO 45 J=1,JEND
    45 CALL PLOTSP(I,J,KMAX,OTIME,D,CON,IDAUX)
    99 OTIME=OTIME+JEND
    ZEROS=.TRUE.
C= THE FOLLOWING PROCEDURE (UP TO STATEMENT 46) IS
C= REQUIRED FOR CASES THAT HAVE A CONSTANT BACKGROUND
    IF(.NOT.CONST)GO TO 46
    TEST=WAVE
    WAVE=.FALSE.
C= HERE WE EVALUATE THE SPACE IN BETWEEN SIGNAL BURSTS AT
C= INTERVALS OF A 1000 DTS AT A TIME,UNTIL THE SEPERATION IS
C= <1000.THEN WE JUMP TO 47 AND EVALUATE NORMAL SEPERATION.
    50 IOLAP=JEND-1000
    IF(IOLAP)47,47,49
    49 ZEROS=.TRUE.
C= CALL ON THE SIGS ROUTINE UNDER THE ZEROS CONDITION
C= BECAUSE MAX ARRAY SIZE IS 1000 WE EVALUATE FOR MAXIMUMS
C= OF 1000 DTS AT A TIME.
    CALL SIGS(AMP,1000,IQ,IR1,IR2,D,CON,AME,FO,WAVE,CONST,CONS)
    ZEROS=.FALSE.
C= CALL ON THE IDEAL PROCESSOR
    IF(THEORY)CALL IDEAL(1000,IPOINT,ITAU,IQA,IP,NTOT,MTOT,IR,DEAD)
    JEND=IOLAP
    DO 51 J=1,1000
   IF(PLOTS) CALL PLOT(M,J,KMAX,OTIME,D,CON,IDAUX)
    R(J)=0
    ICR(J)=0
    S(J)=0
    51 TC(J)=0
    IF(DONE) GO TO 998
    GO TO 50
    47 ZEROS=.TRUE.
C= CALL ON THE SIGS ROUTINE UNDER THE ZEROS CONDITION
    CALL SIGS(AMP,JEND,IQ,IR1,IR2,D,CON,AME,FO,WAVE,CONST,CONS)
    WAVE=TEST
    ZEROS=.FALSE.
     46 IF (THEORY)CALL IDEAL(JEND,IPOINT,ITAU,IQA,IP,NTOT,
-  MTOT,IR,DEAD)
```

```
      ZEROS=.FALSE.
      IF(.NOT.CONST)GO TO 35
      DO 40 J=1,JEND
      IF(PLOTS)CALL PLOT(M,J,KMAX,OTIME,D,CON,IOAUX)
      R(J)=0
      TCR(J)=0
      S(J)=0
   40 TC(J)=0
C-    CALL ON THE SIGS ROUTINE TO COMPUTE A SIGNAL BURST
   35 CALL SIGS(AMP,KMAX,IQ,IR1,IR2,D,CON,AME,FO,WAVE,CONST,CONS)
      IF(DONE) GO TO 998
      OTIME=RANO(1,JV,G2)*FAC+OTIME
      IF((KMAX+OTIME).LT.OTIME)GO TO 25
C-    **** THIS BRANCH IS USED FOR THE OVERLAP CONDITION
C-                    OF SIGNAL BURSTS****
      INTER=OTIME-OTIME
      INSECT=.TRUE.
      IF (THEORY)CALL IDEAL(INTER,IPOINT,ITAU,IQA,IP,NTOT,MTOT,
     IR,DEAD)
      DO 41 J=1,INTER
      IF(PLOTS)CALL PLOT(M,J,KMAX,OTIME,D,CON,IOAUX)
      IC(J)=0.
   41 R(J)=0.
      IF(DONE) GO TO 998
      INSECT=.FALSE.
      K=0
      IVAL=INTER+1
      DO 40 J=IVAL,KMAX
      K=K+1
      S(K)=S(J)
      S(J)=0.
      IC(J)=0.
   40 R(J)=0.
      GO TO 10
C-    ****THIS BRANCH IS USED FOR THE NON-OVERLAP
C-                    CONDITION OF SIGNAL BURSTS****
   25 IF(THEORY)CALL IDEAL(KMAX,IPOINT,ITAU,IQA,IP,NTOT,MTOT,IR
     ,DEAD)
      DO 60 J=1,KMAX
      IF(PLOTS)CALL PLOT(M,J,KMAX,OTIME,D,CON,IOAUX)
      IC(J)=0.
      S(J)=0.
   60 R(J)=0.
      IF(DONE) GO TO 998
      INTER=KMAX
   10 OTIME=INTER+OTIME
      GO TO 999
  998 TOTIME=IDT\*DT
      PERME =NTOT/TOTIME
      WRITE(IOUT,INP)
      IF(DONE) WRITE(IOUT,100)NTOT,MTOT
  100 FORMAT(//" THE NTOT= ",I20,//" THE MTOT= ",I20)
      IF(DONE)STOP
      WRITE(IOUT,120)
      WRITE(IOUT,110)(MKX(I),I,I=1,IP)
  110 FORMAT(5(2X,I7,",I="I2))
  120 FORMAT(//" ACCUMULATOR SUM FOR I=1,IP IN N(K)N(K-I)"/)
      STOP
      END
      SUBROUTINE SIGS(AMP,KMAX,IQ,IR1,IR2,D,CON,AME,FO,WAVE,CONST,CONS)
      DIMENSION M(50)
      LOGICAL WAVE,CONST,ZEROS
      COMMON S(1000),TC(1000),X(47),JV
      COMMON /IDEA/IC(1000),ZEROS,BUIL(2011)
      COMMON /THLOR/R(1000),GE
      COMMON /ADD/MAXC,G1,G2
      SS1=0.
      DT=D*CON/KMAX
      TS=D*CON/2.0
      IF((.NOT.ZEROS).AND.WAVE)S(1)=EXP(-2.*TS**2/D**2)*(1.+AME*
     COS(6.283185*F(*TS))*AMP+S(1)
```

```
      IF(CONST)S(1)=CONS+S(1)
      IVAL=2*IQ+1
C-    IMPULSE RESPONSE OF PMT FROM -IQ TO +IQ
      DO 10 I=1,IVAL
      J=I-IQ-1
   10 H(I)=(1-ABS(FLOAT(J)/IQ))/(IQ*DT)*GE
      Z=RAND(IR2,JV,G2)
      DO 20 K=2,KMAX
      T=(K-1)*DT+TS
C-    IF THIS ISNT A FILLER(ZEROS CONDITION),AND WE WANT THE
C-    CLASSICAL WAVEFORM THEN CALCULATE LAMBDA.
      IF((.NOT.ZEROS).AND.WAVE) S(K)=EXP(-2.*T**2/D**2)*(1.+AME*
     COS(6.283185*FI*T))*AMP+S(K)
C-    IF THERE IS A CONSTANT BACKGROUND THEN ADD IT INTO LAMBDA
      IF (CONST)S(K)=CONS+S(K)
      SS2=(DT*(S(K)+S(K-1))/2.0)+SS1
C-    CALCULATE THE INTEGRAL
      SH=(SS1+SS2)/2.0
C-    ADD UP THE PHOTONS USING THE CLASSICAL WAVEFORM
C-    THIS IS THE RANDOM PHOTON COUNT (TC)
    1 IF(Z.GT.SH)GO TO 20
      TC(K-1)=TC(K-1)+1
      Z=Z+RAND(1,JV,G2)
      GO TO 1
   20 SS1=SS2
   50 DO 50 I=1,KMAX
      IF (IR1.EQ.4)GO TO 51
      MAX=TC(I)
      TCR(I)=0.0
      IF(MAX.EQ.0)GO TO 50
C-    IF WANT TO MAKE RANDOM PHOTOELECTRON HEIGHTS,INSTEAD
C-    OF A CONSTANT SET IR1 TO OTHER THAN 4.
      DO 60 J=1,MAX
   60 TCR(I)=RAND(IR1,JV,G1)+TCR(I)
   51 IF (IR1.EQ.4)TCR(I)=TC(I)
   50 CONTINUE
      IVAL=IQ*2+1
C-    CALCULATE THE SIMULATED SIGNAL BURST
      DO 30 L=1,KMAX
      DO 40 I=1,IVAL
      J=I-IQ-1
      IF((L-J).LT.1.OR.(L-J).GT.KMAX)GO TO 40
      R(L)=H(I)*TCR(L-J)+R(L)
   40 CONTINUE
   30 CONTINUE
      RETURN
      END
      FUNCTION RAND(I,J,G)
C-    THIS FUNCTION ROUTINE IS USED TO CALCULATE A RANDOM VARIABLE
C-    DEPENDING ON THE FIRST INPUT VALUE (I),
C-          FOR I= 1 , CALCULATE AN EXPONENTIAL R.V.
C-               = 2 , CALCULATE A RAYLIEGH R.V.
C-               = 3 , CALCULATE A GAUSIAN R.V.
C-               = 4 , GIVE A CONSTANT=1.0
      J=2051*J
      J=MOD(J,4194304)
      X=J/4194304.0
      GO TO (1,2,2,4),I
    4 RAND=1.0
      RETURN
    1 RAND=ALOG(1./X)
      RETURN
    2 RAND=SQRT(-2.*ALOG(X))*SQRT(2/3.14159265)
      IF(I.EQ.2)RETURN
      RAY=RAND
      J=2051*J
      J=MOD(J,4194304)
      X=J/4194304.0
      RAND=G*(RAY*COS(6.2831853*X))/SQRT(2/3.14159265)+1.0
      RETURN
      END
```

```
3580*   SUBROUTINE IDEAL(INUM,IPOINT,ITAU,IQ,IP,NTOT,MK,IR,DEAD)
3590*C- THIS SUBROUTINE SIMULATES AN IDEAL PROCESSOR
3600*   LOGICAL ZEROS,INSECT,DEDTIM,ONE,DONE
3610*   COMMON /SINE/MAX(20),ONE,DONE,IDTV,IDTIDT,MNTOT
3620*   COMMON /IDEA/TC(1000),ZEROS,N(2000),ITCR(10),INSECT
3625*   COMMON BUL1(1000),TC(1000),BUL2(48)
3628*   COMMON /ADD/MAXC,G1,G2
3630*   INTEGER DEAD
3640*   NUM=INUM
3650*   I=0
3660*C- ON THE ZEROS CONDITION(SPACE BETWEEN THE BURSTS) COMPUTE
3670*C- MTOT WITH VALUES OF ZERO
3680*   IF (ZEROS)GO TO 9
3690*   IF(IR.EQ.0)GO TO 1
3700*   IF(INSECT)NUM=NUM+KMAX
3710*   DO 2 J=1,NUM
3720*   J1=NUM-J+1
3730*   2 TC(J1+IR)=TC(J1)
3740*   DO 3 J=1,IR
3750*   3 TC(J)=ITCR(J)
3760*   IF(INSECT)NUM=NUM-KMAX
3770*   1 NUM=NUM+IR
3780*   I=MOD(NUM,ITAU)
3790*   IF(I.EQ.0)GO TO 4
3800*C- IF DIVISION RESULTS IN A REMAINDER (I) THEN SOME
3810*C- OF THE RANDOM PHOTON COUNT ARRAY (TC) HAS TO
3820*C- BE SAVED AND THEN USED ON THE NEXT CALL TO IDEAL
3830*   DO 5 J=1,I
3840*   5 ITCR(J)=TC(NUM-I+J)
3850*   4 IR=I
3860*   NKMAX=NUM/ITAU
3870*   IF(NKMAX.EQ.0)RETURN
3880*   IVAL=NKMAX+IPOINT-1
3890*   DO 30 K=IPOINT,IVAL
3900*   DO 35 I=1,ITAU
3910*   IF(DEDTIM)GO TO 33
3920*C- IF A DEAD TIME CONDITION EXISTS THEN SKIP THE SUM
3930*C- OF N(K) FOR THIS DT
3940*   IPHOTS=TC(I+(K-IPOINT)*ITAU)
3950*   IF(IPHOTS.GT.MAXC)IPHOTS=MAXC
3960*C- MAXC PHOTONS IS THE LIMIT OF THE COUNTER IN THE
3970*C- IDEAL PROCESSOR
3980*   IF(IPHOTS.GE.1.AND.DEAD.GT.0)DEDTIM=.TRUE.
3990*C- IF A DEAD TIME FROM SATURATION IS TO BE EVALUATED,AND THE
4000*C- THRESHOLD OF 1 PHOTON IS CROSSED THEN SET THE LOGICAL
4010*C- DEDTIME CONDITION AND SKIP DEAD NUMBER OF DT'S
4020*   N(K)=N(K)+IPHOTS
4030*   GO TO 35
4040*   33 IDT=IDT+1
4050*   IF(IDT.LT.DEAD)GO TO 35
4060*   IDT=0
4070*   DEDTIM=.FALSE.
4080*   35 CONTINUE
4090*   30 CONTINUE
4100*   GO TO 20
4110*   9 IF(IR.EQ.0)GO TO 10
4120*   NUM=NUM+IR
4130*   DO 12 J=1,IR
4140*   12 N(IPOINT)=N(IPOINT)+ITCR(J)
4150*   10 IF(NUM.GE.IP)GO TO 14
4160*   DO 11 J=IR+1,NUM
4170*   11 ITCR(J)=0
4180*   IR=NUM
4190*   N(IPOINT)=0
4200*   RETURN
4210*   14 I=MOD(NUM,ITAU)
4220*   IF(I.EQ.0)GO TO 16
4230*   DO 13 J=1,I
4240*   13 ITCR(J)=0
4250*   16 IR=I
4260*   NKMAX=NUM/ITAU
```

```
      IVAL=NKMAX+IPOINT-1
      DO 15 K=IPOINT,IVAL
   15 N(K)=0
   20 IPOINT=IPOINT+NKMAX
      DO 40 L=1,IPOINT
      IF((L-IP).LT.1)GO TO 44
C-    CORRELATION SUM CALCULATED FOR VARYING IP IF ONE
C-    CONDITION IS .FALSE.
      IF(UNE)GO TO 43
      DO 42 J=1,IP
   42 MRX(J)=MRX(J)+N(L)*N(L-J)
   43 IF((L-IQ).LT.1)GO TO 44
      MK=N(L)*(N(L-IP)-N(L-IQ))+MK
   44 IDTV1=L*ITAU
      IF(IDTV1+IDTV.GE.IDTTOT)GO TO 99
  NTOT=NTOT+N(L)
  IF(NTOT.GE.MNTOT)GO TO 99
  40 CONTINUE
      DO 45 K=1,IP
      KI=IPOINT-IP+K
   45 N(K)=N(KI)
      IPOINT=IP+1
      DO 50 K=IPOINT,KI
   50 N(K)=0
      IDTV=IDTV+IDTV1
      RETURN
   99 DONE=.TRUE.
      IDTV=IDTV+IDTV1
      RETURN
      END
      SUBROUTINE PLOT(M,J,KMAX,DTIME,D,CON,IAUX)
C-    THIS SUBROUTINE IF CALLED WILL PLOT :
C-      THE CLASSICAL SIGNAL (.)
C-      THE SIMULATED SIGNAL (*)
C-      AND THE RANDOM PHOTON COUNT (*)
      COMMON /THOR/R(1000)
      COMMON S(1000),IC(1000),X(47),JV,PHI,PLO
      M=M+1
      SVAL=S(J)
      RVAL=R(J)
      IF(SVAL.LT.PLO)SVAL=PLO
      IF(SVAL.GT.PHI)SVAL=PHI
      IF(RVAL.LT.PLO)RVAL=PLO
      IF(RVAL.GT.PHI)RVAL=PHI
      MS=(50./(PHI-PLO))*SVAL+1
      MSS=(50./(PHI-PLO))*RVAL+1
      IF(MS.GT.47)MS=47
      IF(MSS.GT.47)MSS=47
      JMAX=MSS
      IF(MS.GT.MSS)JMAX=MS
      MC=IC(J)
```

```
      LOW1=MC+1
      KHIGH=JMAX-1
      DO 80 K=LOW1,KHIGH
   80 X(K)=1H
      X(MS)=1H.
      X(MSS)=1H*
      IF(MC.EQ.0)GO TO 95
      DO 90 K=1,MC
   90 X(K)=1H*
   95 IF(M.EQ.5)GO TO 25
      HEAD=1HI
      WRITE(IAUX,35)R(J),HEAD,(X(K),K=1,JMAX)
   35 FORMAT(1X,E10.4,13X,48A1)
      GO TO 70
   25 HEAD=1H+
      T=(J+DTIME)*D*CUN/KMAX
      WRITE(IAUX,45)R(J),T,HEAD,(X(K),K=1,JMAX)
   45 FORMAT(1X,E10.4,3X,E10.4,48A1)
      M=0
   70 RETURN
      END
      SUBROUTINE PLOTSP(M,J,KMAX,DTIME,D,CUN,IAUX)
C-    THIS SUBROUTINE PLOTS SPACE (FILLER) IN BETWEEN HURSIS
      M=M+1
      IF(M.EQ.5)GO TO 25
      WRITE(IAUX,55)
   55 FORMAT(1X,"      0.000                 1")
      GO TO 70
   25 T=(J+DTIME)*D*CUN/KMAX
      WRITE(IAUX,45)T
   45 FORMAT(1X,"      0.000",3X,E10.4,"+4")
      M=0
   70 RETURN
      END
```

APPENDIX C

VARIANCE OF THE DUAL CORRELATE AND SUBTRACT ESTIMATOR

In this appendix we wish to determine a formula for the mean-square deviation of the estimate $\hat{M}_{pq}$ defined in the text equation (56) at value of delay (near $T_m/4$ where the expected value of $\hat{M}_{pq}$ is zero. It was our hope to do this for the general signal model which we have presented. To complete such a task requires the use of fourth-order moments of the classical signal process $\lambda(t)$, and it was for this reason that the derivation in the last part of Appendix A was undertaken. We did not have time during the contract period to evaluate and use the fourth order moments of the general signal. For this reason we have restricted this analysis to the case where steady background light is the predominant source of variability error. (Steady light adds variability error even though it cancels in the mean.) This simplifies the problem because of the simplicity of the fourth order moment equations for steady light (homogeneous Poisson counting process).

We define $\hat{M}_{pq}$ here as*

$$\hat{M}_{pq} = \sum m_k \tag{C1}$$

$$m_k = n_k n_{k+p} - n_k n_{k+q}$$

where the summations will all be from 1 to N unless otherwise noted. We have

$$\langle m_k \rangle = \langle n_k \rangle \langle n_{k+p} \rangle - \langle n_k \rangle \langle n_{k+q} \rangle \tag{C2}$$

$$= \bar{n}^2 - \bar{n}^2 = 0$$

*This derivation was performed with plus signs in the delay subscripts instead of minus signs. There is no difference in the results.

where $\bar{n} = \lambda\Delta\tau = \eta\Delta\tau P/h\nu$. From (C2) we have

$$\langle \hat{M}_{pq} \rangle = 0 \tag{C3}$$

we wish to evaluate var $(\hat{M}_{pq}) = \langle \hat{M}_{pq}^2 \rangle - \langle \hat{M}_{pq} \rangle^2 = \langle \hat{M}_{pq}^2 \rangle$

$$\langle \hat{M}_{pq}^2 \rangle = \sum\sum \langle m_i m_j \rangle = \sum \langle m_i^2 \rangle + \sum_{i \neq j} \sum \langle m_i m_j \rangle \tag{C4}$$

In (C4) the product of sums was expanded and the order of expectation and summation interchanged. The $i = j$ terms are separated because they behave differently.

The terms in the first summation give

$$\langle m_i^2 \rangle = \langle n_i^2 n_{i+p}^2 \rangle - 2\langle n_i^2 n_{i+p} n_{i+q} \rangle + \langle n_i^2 n_{i+q}^2 \rangle \tag{C5}$$

$$= \langle n_i^2 \rangle [\langle n_{i+p}^2 \rangle + \langle n_{i+q}^2 \rangle - 2\langle n_{i+p} \rangle \langle n_{i+q} \rangle]$$

$$= (\bar{n} + \bar{n}^2)(2(\bar{n} + \bar{n}^2) - 2\bar{n}^2) = 2\bar{n}^2 + 2\bar{n}^3$$

where the theory of homogeneous Poisson processes has allowed the factorization due to independent of nonoverlapping count intervals* and from which we know that

$$\langle n_i^2 \rangle = \bar{n} + \bar{n}^2 \tag{C6}$$

Next we must evaluate the $i \neq j$ terms in (C4). There are $N^2 - N$ such terms but many of them are zero. We have

---

*At this point for the general nonsteady signal evaluate $\langle m_i^2 \rangle$ with $\lambda(t)$ conditionally given and then evaluate fourth order moments of the process $\lambda(t)$ which is also Poisson.

$$\langle m_i m_j \rangle = \langle n_i n_{i+p} n_j n_{j+p} \rangle - \langle n_i n_{i+q} n_j n_{j+p} \rangle \qquad \text{(C7)}$$

$$- \langle n_i n_{i+p} n_j n_{j+q} \rangle + \langle n_i n_{i+q} n_j n_{j+q} \rangle$$

When all the subscripts are unequal we obtain

$$\langle m_i m_j \rangle = \bar{n}^4 - \bar{n}^4 - \bar{n}^4 + \bar{n}^4 = 0$$

We are restricted to $i \neq j$ and $p \neq q \neq 0$. If we examine the matrix of products $m_i m_j$, the only allowable products for which some of the subscripts of n in (C7) are equal, excluding the i=j case, are found on diagonals parallel to the i=j diagonal. These diagonals are $i = j \pm q$, $i = j \pm p$, and $i = j \pm (p-q)$. We examine these diagonals separately: for $i = j + q$

$$\langle m_i m_j \rangle = \langle n_{j+q} n_{j+q+p} n_j n_{j+p} \rangle - \langle n_{j+q} n_{j+2q} n_j n_{j+p} \rangle \qquad \text{(C8)}$$

$$- \langle n^2_{j+q} n_{j+q+p} n_j \rangle + \langle n^2_{j+q} n_{j+2q} n_j \rangle$$

$$= \bar{n}^4 - \bar{n}^4 - (\bar{n} + \bar{n}^2)\bar{n}^2 + (\bar{n} + \bar{n}^2)\bar{n}^2 = 0$$

Similarly for $i = j - q$, $i = j \pm p$, the result is zero by subtraction. For the diagonals $i = j \pm (p-q)$, however, we obtain after substitution and evaluation

$$\langle m_i m_j \rangle = -\bar{n}^3 \qquad \text{(C9)}$$

For large N we may neglect end effects and observe that there are approximately 2N terms which result from these two diagonals. We may now evaluate (C4) using (C5) and (C9) as

$$\langle M^2_{pq} \rangle = N(2)(\bar{n}^2 + \bar{n}^3) - 2N\bar{n}^3 \qquad \text{(C10)}$$

$$= 2N\bar{n}^2 = 2N(\lambda \Delta\tau)^2 = \mathrm{Var}(\hat{M}_{pq})$$

This is the desired result.

APPENDIX D

SYSTEM DESIGN OF AN ADVANCED PHOTON COUNTING PROCESSOR FOR LOW-LEVEL LDV SIGNALS

Introduction

A problem confronting us in the present design was one of complexity and cost. A two channel duplication of the AEDC processor [1] with the extra requirements of dual-channel advanced-concept operation would have been prohibitively expensive. To solve this problem we have made several significant changes, some of which utilize the power of a high-speed computer controller.

Design Approach for the Advanced Processor

Major cost savings are associated with exact duplication of circuit layout. For this reason, the dual channel system is designed so that it may be operated either as two completely separate identical units in one rack; or as two independent units with synchronized data (for cross correlations) or as a one channel system with a synchronous normalizing channel (same system clock and n_k sequence but separate delays). The counter/timer (C/T) functions needed for system control were obtained in the AEDC system [1] from a $1500 laboratory counter, selected because of the availability of options ($285) for computer control and read. It is considerably less expensive to include the C/T functions in the special-purpose hardware to avoid both the cost of two units ($3570) and the associated computer cables, I/O cards, etc. This puts an even more stringent requirement on reducing complexity of other circuits to give more room on the wire wrap panel (162-180 IC sockets unless multiple panels are used). The following system concepts have been incorporated.

1. Eliminate all front panel controls and displays. The system thus utilizes the display and command of the controlling mini-computer and cannot function separately. This saves LED driver integrated circuits as well as the front panel itself.
2. Use a newer, lower cost voltage variable oscillator for the system clock.
3. Replace the laboratory counter with ECL counter/timer (C/T) circuits.
4. Use an external, separate heavy duty ECL power supply (≈ 16 Amps) to save space in the system enclosure and avoid a large heat source in the enclosure.
5. Reduce the maximum count to 3 bits instead of 4 (see following justification). This simplifies all of the circuits and reduces package count.
6. Reduce the number of control and read data circuits. (See following discussion.)
7. Do not require the 3 bit counter to be selectively saturable. Let it saturate at 7 (111).
8. Remove the single-clipper circuit and the associated multiplexer.
9. Limit the accumulator to 15 bits + sign to be compatible with the 16 bit word of the computer. Read the accumulator often enough to avoid overflow.
10. Replace the 4 bit subtractor with a 3 bit subtractor adder. The add function could be used in one of the normalization schemes.
11. Include an experimental analog servo loop for zero adjusting the system clock to the proper multiple of the mean signal frequency.

Reduction of Counter Bit Number

The maximum periodic rate of discriminator output pulses is 120 MHz (dead time > 8nsec). The largest random rate is usually less, say 70 MHz. In order for the count of 7 to be executed therefore, we assume the count interval to be larger than 0.1 μsec ($1/f_o$ > 0.4 or 0.8 μsec depending on the delay choices). Thus we may have the count exceeded for signal frequency f_o < 2.5 MHz or 1.25 MHz. We observe, however, that a

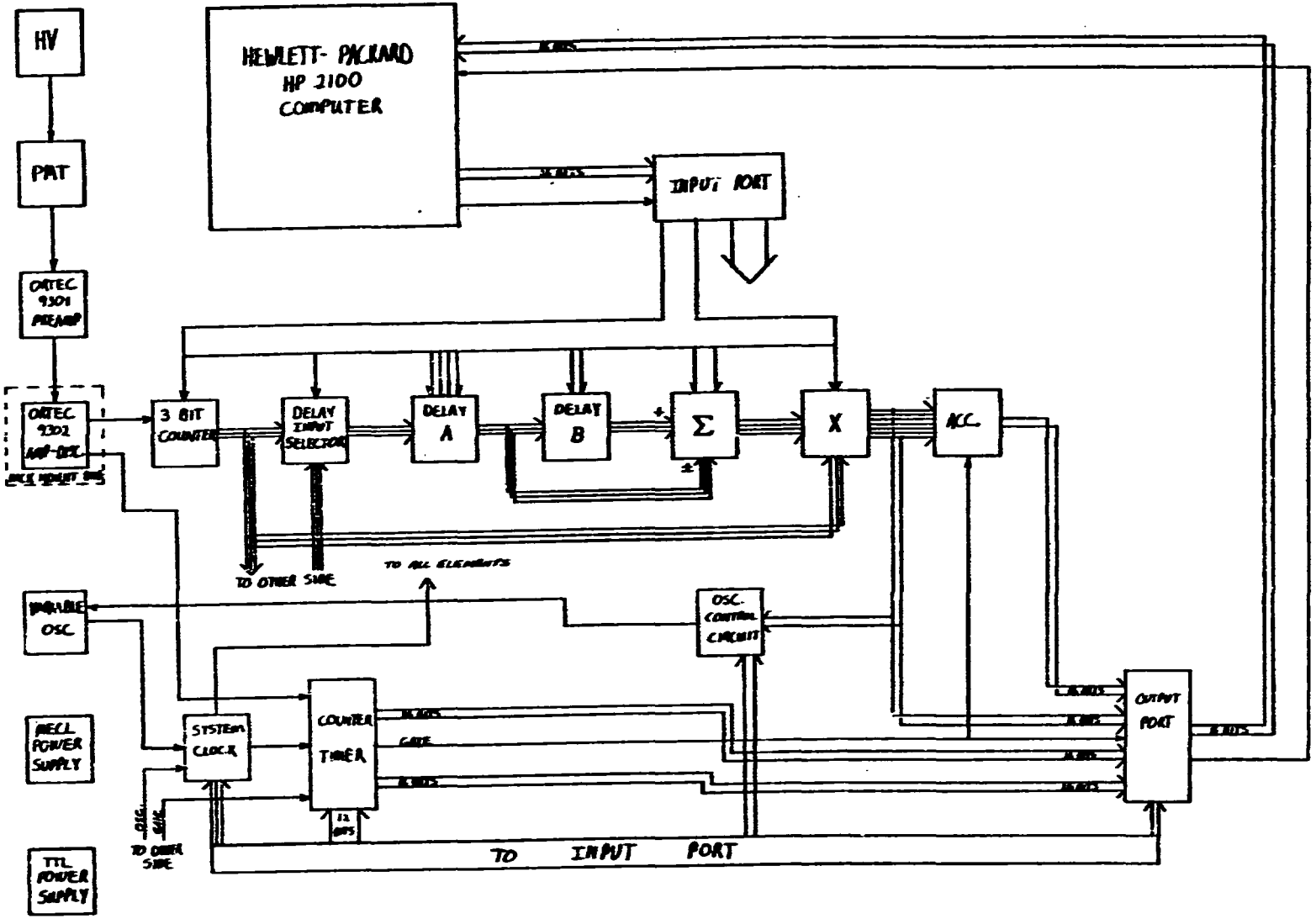

Figure D1. System Diagram for one of two identical connected sections of a Dual Channel Photon Processor.

count of 7 in a quarter of a cycle is a peak rate of 14 electrons/cycle. This is where the burst counter can become useful. Thus a 3 bit counter is adequate because when larger signals are present a burst counter processor should be used. If the larger signals are unwanted because they occur from larger particles, then saturating the count at 7 will reduce their effect in favor of smaller signals.

Read logic for photon statistics.- The 16 bit word length and the high speed of the H.P. 2100 computer will allow straight forward READ circuitry. Each channel will have a 16 bit T^2L latch connected to the 15 bit plus sign accumulator. In order that the counter/timer and the multiple interval statistics may be read, selectable steering gates will be used so that the first 6 bits can be connected to the output of the multiplier. Sequential numbers may then be read as follows:

1. Set maximum delay in A+B and set one side of multiplier to 1.
2. Run data and clock.
3. Stop clock.
4. Read multiplier out with commanded single clock advance.

This will produce a string of more than 20 sequential numbers. In order to read the C/T total (8 digits) 32 bits is required (BCD code). This will be accomplished by sequentially reading two 16 bit words time-multiplexed to the TTL output port.

Description of Circuits

This section describes the subsystem circuits and components which comprise the dual channel photon processing system one channel of which is shown in Figure D1.

External subsystems.- The external subsystems are the following:

1. Two photomultiplier tubes and associated housings and power supplies.

2. Six precision 50 Ω connecting cables.
3. Two preamps.
4. Two amplifier/discriminators.
5. One NIM bin (rack mounted).
6. Two voltage controllable oscillators (1-200 MHz)
7. Two rack-mounted integrated circuit power supplies and connecting cables.
8. A computer with two microcircuit I/O cards (16 bits in and 16 bits out for each with device command line and device-ready flag line), and two 36 pair twisted lead cables with connectors.

Three bit counter.- This is a dual section counter which stops and holds the count of seven instead of turning over to zero and continuing. Two counter sections alternate so that one may have data transferred and be reset while the other one is counting. In order to avoid the possibility of counting a border line event twice, a dead time between count intervals approximately 2 nsec will be incorporated. The dead time between input pulses (from the discriminator) will be $\leq$ 10 nsec with a design objective of 8 nsec. The alternate count intervals will be equal (design objective). A control bit allows the counter output to the delays to be set to zero (data gate).

Delay sections.- The two delay sections A and B are specified as A = {0,1,2,3,4,5,6,8,9,10,11,12} and B = {0,2,4,8}. This set allows sequential autocorrelations with delays up to 20 in addition to the dual correlate and subtract and the normalizing modes.

For dual channel operation with one channel normalizing, a multiplexer is provided which allows the data from the other channel counter to be selected as delay input. Since the separate channels are identical physically, each has an input and an output to the other channel.

Four control bits select the A delay. Two control bits select the B delay. An additional bit selects the output of the other data channel instead of the counter output of this channel.

Adder/subtractor & mode selector.- In the AEDC unit an option for subtracting a constant from each n_k was included. The purpose was to avoid overflowing the accumulator in auto-correlate mode when a signal with large mean is encountered. The ability of the computer for high-speed read to DMA avoids the necessity of subtracting a constant, since the accumulator may be read often to avoid overflow. The two control bits allow selection of add, subtract, or add zero. The adder subtractor output is four magnitude bits plus sign.

Multiplier.- The multiplier has seven bits plus sign out. A control bit allows the undelayed path input to be set to 001 instead of n_k.

Accumulator.- The accumulator has 15 bits plus a sign bit. It can be reset by a single pulse. It will be implemented in 2's complement; the computer software will convert to sign and magnitude. The reset pulse must also transfer the accumulator values to latches in the output port to the computer.

Counter/timer.- This section replaces the external counter/timer used in the AEDC System. It consists of two 8-decade BCD counters and associated input selectors and controls. Each counter may select as input either the precision 1 MHz oscillator, the system clock, or the second discriminator output (external input). A fast prescaler selects divide by 1, 2, or 5 for counter #1. Counter #2 is multiplexed to the 16 bit output port (1st 4 significant decades and 2nd 4 significant decades separately selectable.) The first counter produces output pulses at decade counter #1 selector. The package count does not include multiplexing and read outputs for counter #2.

A gate generator block does the following: It produces the pulse which is applied to the accumulator and the computer flag; it programably reads and resets the C/T; and it produces a gate pulse between two successive counter #1 output pulses for application to the counter #2 control gates (counter #2 stops and holds when gate goes back down). The programable states include: a) read and reset counter #2 at the entry of the control word (CW) and at each output pulse from counter #1 (PFC); b) read and reset counter #2 CW but not PFC; c) read and reset counter #2 at PFC but not at CW; d) do not read and reset counter #2 at either PFC or CW. (This allows, by software, for counting the photon rate over the duration of an autocorrelation sequence and then stopping at the end of a number of smaller intervals.)

The control bits needed for the C/T are as follows: Three bits are used to select which of 3 inputs goes to each of the two decade counters. (Assumes both will not have same input.) Three bits will select the decade output of the decade scaler (counter #1). Two more bits select the prescale divisor (1, 2, 5). Three bits have been allowed for the four read/reset states (2 bits) and an extra control bit (spare). Finally, there is one bit which allows application of the control gates from the other C/T to the accumulator read/reset line instead of this channel's C/T. (This is for cross correlation with synchronous accumulator read/reset.)

System clock.- The system clock accepts a periodic wave form with 1 positive-going transition per cycle) and shapes this into a periodic pulse train at the ECL voltage levels. It includes buffer gates for proper fan out (5 packages). It includes controls which allow the clock to be stopped cleanly and a one-shot clock pulse generator which can be activated by computer instruction. This feature allows sequential n_k

values to be read out of the system for multiple interval statistics. The control bits are one for on/off and one for single pulse. There is also an ungated clock line which is used as an input to the C/T. There is a control bit which allows the other system clock to be selected (when the other channel data is used, for example).

Output port.- Each channel has one 16 bit TTL compatible output port and a 1 bit flag pulse line. The output port includes a multiplexer (two 16 bit sections of the C/T, the 16 bit accumulator output and a 7 bit output from the multiplier), a 16 bit latch, and ECL to TTL voltage level translators. The output multiplexer requires 2 bits of control to select one of 4 outputs.

At the present time it is not clear which of the following approaches could be utilized: a) all ECL construction with only 17 bits of ECL/TTL translator as the output; b) a separate panel section of TTL circuitry which includes most of the C/T and the output latches for the output port. The b) approach would require less expensive IC's and less power for part of the system. However, the cost of a separate panel and the panel interconnections may make a) preferable.

Oscillator control.- This subsystem provides automatic fine tuning of the variable system clock for the determination of the mean velocity. The mean value of the multiplier output is negative while the clock frequency is too high. Thus the intent here is to use fast digital/analog conversion and analog integration with controllable reset, integration, and hold states to provide a control voltage to the external voltage controllable oscillator. Two control bits are required.

This feature is a research item. It may later prove more advisable to use the D/A converter with a portion of the

computer control word bits so that the mean velocity selection becomes a software task.

Input port.- All machine control is accomplished by 30 bits of information and the time at which certain of the bits are changed. These bits are latched into the processor input port 15 at a time by a single line command pulse from the computer. All time-critical bits of control are included in control word 0. (One of the sixteen bits from the computer is the address of the control word 0 or 1.) Table D1 provides a tentative assignment of control bits. The bit number refers to the power of 2 in standard binary format.

Package count.- An integrated circuit package count estimate of 147 IC's made for one of the two identical channels. The estimate assumes the use of a panel with 162 sockets and design for each subcircuit with the same approach previously developed for the AEDC unit. This leaves 15 spare sockets for flexibility in design and/or additions. A slightly improved approach has also been identified which uses 2 bit arithmetic logic units (ALU) instead of 4 bit ALU's to reduce circuit speed limitations. This approach would actually produce more useable sockets because the panel would have 180 standard sockets instead of 150 plus 12 4 bit ALU sockets.

Address Zero

Bit	Function	Bit	Function
0	Clock Gate	0	C/T Input Selection
1	Clock One Shot	1	
2	3-Bit Counter Gate	2	
3	A Delay	3	C/T Decade Select for Counter #1
4		4	
5		5	
6		6	C/T Prescale Select
7	B Delay	7	
8		8	Adder/Subtractor
9	Multiplier	9	
10	Output Port Multiplex	10	Accumulator Control from Cross Channel
11		11	n_x from Cross Channel
12	Accumulator Reset Control	12	Clock from Cross Channel
13		13	Oscillator Control State
14		14	

TABLE D1. CONTROL WORD FORMAT

REFERENCES

1. W. T. Mayo, Jr., Digital Photon Correlation Techniques, Final Report, USAF Contract F40600-74-C-0016, May 1974 - October 1975, for Arnold Engineering Development Center, Report No. AEDC-TR-76-81, July 1976.

2. Mayo, W. T., Jr., Laser Doppler Flowmeters - A Spectral Analysis, Ph.D. Thesis, Georgia Institute of Technology, Atlanta, Georgia, May, 1969.

3. Allen, J. B., Estimation of the Frequency of Laser Velocimeter Signals, Ph.D. Thesis, Georgia Institute of Technology, January, 1973.

4. Durrani, T. S., Noise Analysis for Laser Doppler Velocimeter Systems, IEEE Transactions, COM-20: 296-307, 1973 (June). See also Durrani, T. S., and Greated, C. A., Statistical Analysis and Computer Simulation of Laser Doppler Velocimeter Systems, IEEE Transactions, IM-22: 23-34, 1973 (March).

5. Yu. N. Dubnitshev, V. P. Koronkevich, V. S. Sobolev, A. A. Stolpovski, Yu. G. Vasilenko, and E. N. Utkin, Laser Doppler Velocimeter as an Optoelectronic Data Processing System, Applied Optics, Vol. 14, No. 1, 180, 1975 (January).

6. Meyers, J. F., Computer Simulation of a Fringe Type Laser Velocimeter. In: Proceedings of the Second International Workshop on Laser Velocimetry, Purdue University, March 27-29, 1974.

7. R. J. Adrian, Statistics of Laser Doppler Velocimeter Signals: Frequency Measurement, J. of Physics E: Scientific Instruments, Vol. 5, 91, 1972.

8. George, W. K. and Lumley, J. L., The Laser Velocimeter and its Applications to the Measurement of Turbulence. Journal of Fluid Mechanics. 60, pt. 2: 321-362, 1973.

9. Snyder, D. L., Random Point Processes. New York, John Wiley and Sons, Inc., 1975.

10. Papoulis, A., Probability, Random Variables and Stochastic Processes. New York, McGraw-Hill. 1965.

11. W. T. Mayo, Jr., Modeling Laser Velocimeter Signals as Triply Stochastic Poisson Processes, in the Proceedings of the Minnesota Symposium on Laser Doppler, University of Minnesota, Bloomington MI, October 1975.

12. H. Z. Cummins and E. R. Pike, Editors, Photon Correlation and Light Beating Spectroscopy, NATO Advanced Study Institute Series, Plenum Press, New York, 1974.

13. E. R. Pike, The Application of Photon-Correlation Spectroscopy to Laser Doppler Velocimeter, The Use of the Laser Doppler Velocimeter for Flow Measurements, Proceedings of a workshop, Purdue University, LaFayette, Indiana, March 1972.

14. T. S. Durrani and C. Greated, Statistical Analysis of Velocity Measuring Systems Employing the Photon Correlation Technique, IEEE Transactions on Aerospace and Electronic Systems, Vol. AES-10, No. 1, 17, 1974 (January).

15. A. D. Birch, D. R. Brown and J. R. Thomas, Photon Correlation Spectroscopy and its Application to the Measurement of Turbulence Parameters in Fluid Flows, J. of Physics D: Appl. Phys. Vol. 8, 438, 1975.

16. J. B. Abbiss, L. J. S. Bradbury, M. P. Wright, Measurements on an Axi-symmetric Jet Using a Photon Correlator, in The Accuracy of Flow Measurements by Laser Doppler Methods, Proceedings of LDA Coppenhagen 1975, P.O.Box 70, DK 2740, Skovlunde Denmark, 1976.

17. T. S. Durrani and C. A. Greated, Spectral Analysis and Cross-Correlation Techniques for Photon Counting Measurements on Fluid Flows, Applied Optics, Vol. 14, No. 3, 1975 (March).

18. C. Fog, A Photon Statistical Correlator for LDA Application, The Proceedings of LDA Symposium, Copenhagen, 1975.

19. E. V. Hoversten, D. L. Snyder, R. O. Harger, and K. Kurimoto, Direct Detection Optical Communication Receivers, IEEE Trans. on Communications, COM-22, No. 1, 17 (January, 1974).

20. Farmer, W. M., The Interferometric Observation of Dynamic Particle Size Velocity, and Number Density, Ph.D. Dissertation, The University of Tennessee. 1973.

21. Bertolotti, M., Photon Statistics, In: Photon Correlation and Light Beating Spectroscopy, H. Z. Cummings and E. R. Pike (ed.) New York, Plenum Press. 1974.

22. R.C.A. Photomultiplier Tube Manual, Technical Series PT-61, RCA Electronic Components, Harrison, N.J. 07029 (1970).

23. W. T. Mayo, Jr., M. T. Shay, and S. Riter, The Development of New Digital Data Processing Techniques for Turbulence Measurements with a Laser Velocimeter, Final Report (AEDC-TR-74-53), USAF Contract No. F40600-73-C-003, August 1974.

24. R. Bracewell, The Fourier Transform and Its Applications, McGraw-Hill, New York, N. Y. 1965.

25. R. H. Forrester, Jr., Phase-Tracking Performance of Direct-Detection Optical Receivers, A Masters' Thesis, Washington University Sever Institute of Technology, St. Louis, Mo. 1973.

26. R. P. Chambers, Random Number Generation, IEEE Spectrum, February 1967, p. 48-56.

"The aeronautical and space activities of the United States shall be conducted so as to contribute . . . to the expansion of human knowledge of phenomena in the atmosphere and space. The Administration shall provide for the widest practicable and appropriate dissemination of information concerning its activities and the results thereof."

—NATIONAL AERONAUTICS AND SPACE ACT OF 1958

NASA SCIENTIFIC AND TECHNICAL PUBLICATIONS

TECHNICAL REPORTS: Scientific and technical information considered important, complete, and a lasting contribution to existing knowledge.

TECHNICAL NOTES: Information less broad in scope but nevertheless of importance as a contribution to existing knowledge.

TECHNICAL MEMORANDUMS: Information receiving limited distribution because of preliminary data, security classification, or other reasons. Also includes conference proceedings with either limited or unlimited distribution.

CONTRACTOR REPORTS: Scientific and technical information generated under a NASA contract or grant and considered an important contribution to existing knowledge.

TECHNICAL TRANSLATIONS: Information published in a foreign language considered to merit NASA distribution in English.

SPECIAL PUBLICATIONS: Information derived from or of value to NASA activities. Publications include final reports of major projects, monographs, data compilations, handbooks, sourcebooks, and special bibliographies.

TECHNOLOGY UTILIZATION PUBLICATIONS: Information on technology used by NASA that may be of particular interest in commercial and other non-aerospace applications. Publications include Tech Briefs, Technology Utilization Reports and Technology Surveys.

Details on the availability of these publications may be obtained from:

SCIENTIFIC AND TECHNICAL INFORMATION OFFICE

NATIONAL AERONAUTICS AND SPACE ADMINISTRATION

Washington, D.C. 20546